DEMONSTRATION REPORT

Demonstration of MPV Sensor at Yuma Proving Ground, AZ

ESTCP Project MR-201005

June 2011

Nicolas Lhomme
Sky Research, Inc

REPORT DOCUMENTATION PAGE

Form Approved
OMB No. 0704-0188

PLEASE DO NOT RETURN YOUR FORM TO THE ABOVE ORGANIZATION.

1. REPORT DATE *(DD-MM-YYYY)*	2. REPORT TYPE	3. DATES COVERED *(From - To)*
27-06-2011	Final Technical Report	September 2010-June 2011

4. TITLE AND SUBTITLE

Demonstration of MPV Sensor at Yuma Proving Ground, AZ: ESTCP MR-201005 Man Portable Vector EMI Sensor for Full UXO Characterization

5a. CONTRACT NUMBER

W912HQ-10-C-0030

5b. GRANT NUMBER

5c. PROGRAM ELEMENT NUMBER

6. AUTHOR(S)

Dr. Nicolas Lhomme, Sky Research, Inc.

5d. PROJECT NUMBER

5e. TASK NUMBER

5f. WORK UNIT NUMBER

7. PERFORMING ORGANIZATION NAME(S) AND ADDRESS(ES)

Sky Research, Inc.
445 Dead Indian Memorial Road
Ashland, OR 9520

8. PERFORMING ORGANIZATION REPORT NUMBER

9. SPONSORING/MONITORING AGENCY NAME(S) AND ADDRESS(ES)

Environmental Security Technology Certification Program
901 North Stuart Street, Suite 303
Arlington, VA 22203-1821

10. SPONSOR/MONITOR'S ACRONYM(S)

11. SPONSOR/MONITOR'S REPORT NUMBER(S)

12. DISTRIBUTION/AVAILABILITY STATEMENT

Approved for public release; distribution is unlimited

13. SUPPLEMENTARY NOTES

14. ABSTRACT

The Man-Portable Vector electromagnetic induction sensor is a new-generation instrument designed to extend classification of unexploded ordnance (UXO) to sites where vegetation or terrain limit access to vehicle-based advanced geophysical platforms. The MPV was tested at Yuma Proving Ground, Arizona UXO Standardized Test Site in October 2010. Most demonstration objectives were attained. Detection objectives were exceeded with 100% target detection within 0.3-meter depth and 90% within 1 meter, zero false alarms from non-metallic objects and no detectable targets missed during field survey. Discrimination goals were met with over 90% correct classification in top 1 meter and recover of location and depth within 0.1 m. False alarm rate for discrimination reached 60% in top 0.3 meter and 75% at 1 meter. The system was remarkably resilient for a second-generation research prototype. Its electromagnetic-beacon positioning system was tested against a Real-Time Kinematic GPS and yielded satisfactory accuracy. The MPV is scheduled to be deployed in June 2011 at next ESTCP demonstration at former Camp Beale, California.

15. SUBJECT TERMS

Man Portable Vector Sensor, Electromagnetic sensors, UXO, YPG

16. SECURITY CLASSIFICATION OF:			17. LIMITATION OF ABSTRACT	18. NUMBER OF PAGES	19a. NAME OF RESPONSIBLE PERSON
a. REPORT	b. ABSTRACT	c. THIS PAGE			Dr, Herb Nelson
UU	UU	Uu	UU		19b. TELEPHONE NUMBER *(Include area code)* 703-696-8726

Reset

Standard Form 298 (Rev. 8/98)
Prescribed by ANSI Std. Z39.18

TABLE OF CONTENTS

LIST OF FIGURES

LIST OF TABLES

ACKNOWLEDGMENT

The MPV demonstration at Yuma Proving Ground, Arizona was funded by the Environmental Security Technology Certification Program project MR-201005. Initial sensor development and testing was supported by Strategic Environmental Research and Development Program project MM-1443. The field deployment involved Dr. Benjamin Barrowes (CRREL-ERDC), David George (G&G Sciences), Jon Jacobson and the P.I. (both from Sky Research). The P.I. was the main performer for all other tasks. Joy Rogalla assisted with project coordination and document editing. Dr. Laurens Beran shared advice on classification strategies. Dr. Stephen Billings and Dr. Barry Zelt reviewed the final report.

EXECUTIVE SUMMARY

The Man-Portable Vector (MPV) sensor is a new-generation instrument designed to extend classification of unexploded ordnance (UXO) to sites where vegetation or terrain limit access to vehicle-based advanced geophysical platforms. The MPV is a handheld electromagnetic induction sensor that consists of a transmitter, an array of three-dimensional receivers and a field-programmable control unit. The MPV is equipped with a portable local positioning system that is based on locating the MPV transmitter, which acts as a beacon when turned on. The method is not affected by natural obstacles, as opposed to commonly used GPS and roving lasers; a survey can therefore be performed in forested and rugged environments. A touch-screen display mounted on the MPV handle provides immediate feedback on signal strength and data quality and facilitates quick switches in operation modes. This functionality can be exploited by collecting detection and discrimination data as part of the same survey. The sensor is first used in dynamic search mode until a target is detected, and switched to static, cued interrogation mode to acquire high quality data for target characterization. The original MPV prototype was rebuilt to improve maneuverability and ruggedness prior to field deployment.

The second-generation MPV was deployed at Yuma Proving Ground, Arizona UXO Standardized Test Site in October 2010 to evaluate its detection and discrimination capabilities. Most of the demonstration objectives were attained. Detection objectives were exceeded with 100% target detection within 0.3-meter depth and 90% within 1 meter, zero false alarms from non-metallic objects and no detectable targets missed during the field survey. Discrimination goals were met with over 90% correct classification in the top 1 meter and correct prediction of location and depth to within 0.1 m. The false alarm rate for discrimination exceeded the 50% objective with 60% in top 0.3 meter and 75% at 1 meter – the stated objective was too ambitious for an artificial site with fourteen potential UXO types and a UXO-to-clutter ratio orders of magnitude greater than that of a live site. A production rate of 100 anomalies per day was met on the Blind Grid; data analysis time was greater than anticipated as new processes had to be developed to analyze new MPV and beacon data; however, data were interpreted and submitted within the required four weeks of survey completion. As part of the evaluation a field geophysicist was trained to utilize the MPV for detection and discrimination; the trainee was operational within hours such that data collection was shared between him and the P.I. for the rest of the survey. The system was remarkably resilient for a second-generation research prototype. For its first field test, the beacon positioning system, which was tested against a Real-Time Kinematic GPS, yielded satisfactory accuracy and only incurred one incident, when cable connectors broke. Occasional survey downtime was due to a conflict in the computer operating system. Both weaknesses have now been addressed.

The YPG tests are the first stage in a series of live site demonstrations that will help establish the performance, limitations and costs of the MPV technology. The YPG demonstration was successful and suggests a strong potential for shallow UXO detection and classification. Today there are no commercially available systems with such capabilities. The MPV and beacon sensor system are scheduled to be deployed and tested in June 2011 at the ESTCP Pilot Discrimination Study at former Camp Beale, California.

ACRONYM LIST

APG	Aberdeen Proving Ground
AZ	Arizona
BTG	Blind Test Grid
BUD	Berkeley UXO Discriminator
cm	Centimeter
CO	Colorado
CRREL	Cold Regions Research and Engineering Laboratory
DAQ	Data Acquisition System
DE	Differential Evolution
DGM	Digital Geophysical Mapping
DoD	Department of Defense
EMI	Electromagnetic Induction
ERDC	Engineering Research and Development Center
ESTCP	Environmental Security Technology Certification Program
GPS	Global Positioning Systems
Hz	Hertz
IDA	Institute for Defense Analyses
m	Meter
mm	Millimeter
MPV	Man Portable Vector
ms	millisecond
NH	New Hampshire
NSMC	Normalized Surface Magnetic Charge
NSMS	Normalized Surface Magnetic Source
NVMS	Normalized volume Magnetic Source
OR	Oregon
Pd	Probability of Detection
Pdisc	Probability of Discrimination
Pfa	Probability of False Alarm
PI	Principal Investigator
POC	Points of Contact
RS	Response Stage
RTK	Real-time Kinematic
s	Second
SERDP	Strategic Environmental Research and Development Program
SKY	Sky Research, Inc.
SNR	Signal to Noise Ratio
TEMTADS	Time Domain Electromagnetic Towed Array Detection System
TNSMS	Total Normalized Magnetic Source
UXO	Unexploded Ordnance
YPG	Yuma Proving Ground

1.0 INTRODUCTION

This report presents the results of the demonstration conducted using the Man Portable Vector (MPV) sensor at the standardized Unexploded Ordnance (UXO) Test Site at Yuma Proving Grounds (YPG) in Arizona (AZ) during October, 2010. This work is being performed under the Environmental Security Technology Certification Program (ESTCP) project MR-201005.

1.1 BACKGROUND

The Fiscal Year (FY) 06 Defense Appropriation contains funding for the "Development of Advanced, Sophisticated, Discrimination Technologies for UXO Cleanup" in the ESTCP. As the Defense Science Board observed in 2003, "The […] problem is that instruments that can detect the buried unexploded ordnance (UXO) also detect numerous scrap metal objects and other artifacts, which leads to an enormous amount of expensive digging. Typically 100 holes may be dug before a real UXO is unearthed! The Task Force assessment is that much of this wasteful digging can be eliminated by the use of more advanced technology instruments that exploit modern digital processing and advanced multi-mode sensors to achieve an improved level of discrimination of scrap from UXO."

ESTCP responded by conducting a Discrimination Pilot Study and funding development of a new generation of geophysical sensors. Results for the first three discrimination studies (at Camp Sibert, Alabama, San Luis Obispo, California, and Camp Butner, North Carolina) were encouraging. In particular, new sensors combined with advanced classification methods allowed the demonstrators to correctly identify a significant fraction of the anomalies as arising from non-hazardous items that could be safely left in the ground. Such performance was facilitated by favorable survey conditions, vegetation, and modest topographical variations that permitted deployment of vehicular and cart-based geophysical platforms.

The results from these studies are encouraging; however, there are many Department of Defense (DoD) sites where terrain and vegetation limit the use of large wheel-based sensor systems. Terrain and vegetation conditions (e.g., dense forests and steep terrain) at many sites also preclude use of traditional location systems like global positioning system (GPS) and laser. These systems can fail at sites when terrain and vegetation interfere and line-of-sight surveying is not possible.

1.2 OBJECTIVE OF THE DEMONSTRATION

The overarching goal of this ESTCP demonstration is to validate the MPV technology for UXO characterization at sites where difficult topography and vegetation preclude deployment of wheel-based advanced geophysical platforms and traditional "line-of-sight" positioning methods (e.g. GPS, laser). The objective is to measure the performance of the MPV for UXO detection and discrimination at a site designed for evaluating the depth of investigation as a function of the target size and type. The effectiveness of survey protocols and the ease of use of the technology also will be assessed. This particular phase of the demonstration was performed at the Standardized Test Site at the YPG where many UXO detection technologies are tested before validation by DoD.

Successful deployment of the MPV will extend advanced discrimination capabilities to sites with challenging surveying conditions and, thus allow for advanced discrimination to be applied at most human trafficable land locations at moderate cost. The system is deployed in conjunction with a portable local positioning system free from "line-of-sight" requirements.

The MPV is a programmable, wide-band, time-domain, Electromagnetic Induction (EMI) sensor comprised of a single transmitter coil and an array of multi-component receivers. The MPV prototype was developed and characterized by the Engineering Research and Development Center-Cold Regions Research and Engineering Laboratory (ERDC-CRREL) (Dartmouth, New Hampshire [NH]) under the Strategic Environmental Research and Development Project (SERDP) project MM-1443. Extensive laboratory tests and preliminary field trials confirmed its potential to extend classification capabilities to man-portable systems. In preparation for substantial field deployments, the sensor head and operating software were modified in 2009-2010 to improve portability, solidity and usability. The associated positioning system operates on the principle of monitoring the primary field of the MPV transmitter, acting as a beacon, with a pair of EMI receivers mounted on a portable base station place near the anomaly of interest. The beacon system predicts the MPV position and orientation within 1 centimeter (cm) and 1 degree, respectively, out to distances of 5 meters (m). With the combination of a multi-component EMI sensor and accurate positioning, we anticipate achieving excellent discrimination performance of shallow targets with a productivity rate on the order of one hundred anomalies per day.

1.3 REGULATORY DRIVERS

The Defense Science Board Task Force on UXO noted in its FY06 report that 75% of the total cost of a current clearance is spent on digging scrap. A reduction in the number of scrap items dug per UXO item from 100 to 10 could reduce total clearance costs by as much as two-thirds. Thus, discrimination efforts focus on technologies that can reliably differentiate UXO from items that can be safely left undisturbed.

Discrimination only becomes a realistic option when the cost of identifying items that may be left in the ground is less than the cost of digging them. Because discrimination requires detection as a precursor step, the investment in additional data collection and analysis must result in enough fewer items dug to pay back the investment. Even with perfect detection performance and high Signal-to-Noise Ratio (SNR) values, successfully sorting the detections into UXO and non-hazardous items is a difficult problem but, because of its potential payoff, one that is the focus of significant current research. This demonstration represents an effort to transition a promising discrimination technology into widespread use at UXO-contaminated sites across the country.

2.0 TECHNOLOGY

The MPV technology is based on a man-portable EMI sensor with a transmitter coil and a set of vector receivers. The system tested at YPG is the second generation prototype MPV.

2.1 MPV TECHNOLOGY DESCRIPTION

The MPV is a man-portable, wide-band, time-domain, EMI sensor composed of a single transmitter coil and an array of five receiver units that measure all three components of the EM field. The sensor was specifically designed to (1) be man portable and therefore easier to deploy, maneuver and adapt to a survey environment, and (2) acquire data that is suitable for discriminating UXO from non-UXO targets. The MPV sensor head for this demonstration comprises a 50-cm-diameter circular loop transmitter coiled around a disk that intermittently illuminates the subsurface, and five multi-component receiver units (cubes) that measure the three orthogonal components of the transient secondary EM field decay with three air-induction 8-cm square coils. One receiver cube is co-axial with the transmitters while four receivers are placed off-axis around the transmitter loops in a cross pattern (Figure 1). Gasperikova et al (2007) and others have shown that having multi-component receivers placed at multiple locations can help reduce the ambiguity between the size and depth of a buried target by more readily allowing recovery of the components of the polarizability tensor associated with a buried metallic object, an indicator of the target shape.

The MPV is a programmable instrument. The duration of the excitation and time decay recording can be adjusted to any given time to accommodate survey needs. The MPV features distinct operating modes for detection and discrimination with a seamless switch between the two. Detection mode consists of dynamic data collection for digital geophysical mapping (DGM). It is based on fast EMI transmit-receive cycles so that the sensor can continuously move (e.g., 1 millisecond [ms] time decay, similar to Geonics EM-61). Discrimination mode is tailored for optimizing data quality and the ensuing target characterization. The sensor is static so that signals can be stacked (averaged to reduce noise); longer EMI cycles are applied to capture variations in time decay rates (e.g., 25 ms, similar to Geonics EM-63). This late-time information has been shown to be very useful for estimating target shape (Billings et al., 2007). Other currently available systems with multiple time channel measurement capabilities (e.g., Berkeley UXO Discriminator [BUD], Geonics EM63, Time Domain EM Towed Array Detection System [TEMTADS]) are required to be mounted on a cart platform due to the size and weight of the multiple coils of wire required for the transmitters and receivers.

The MPV user interface has real-time monitoring and feedback capabilities on data quality, spatial coverage and other key features (signal intensity, time decay, secondary targets, and presence of magnetic soil). For example, the interface includes a target location tool obtained by displaying the direction and amplitude of the measured EMI field at each receiver unit (the so-called “dancing arrows” in Figure 2). All these features assist the field operator in efficient data collection, so that detection and discrimination data can be collected as part of the same survey, thus limiting the need to revisit an anomaly for further characterization.

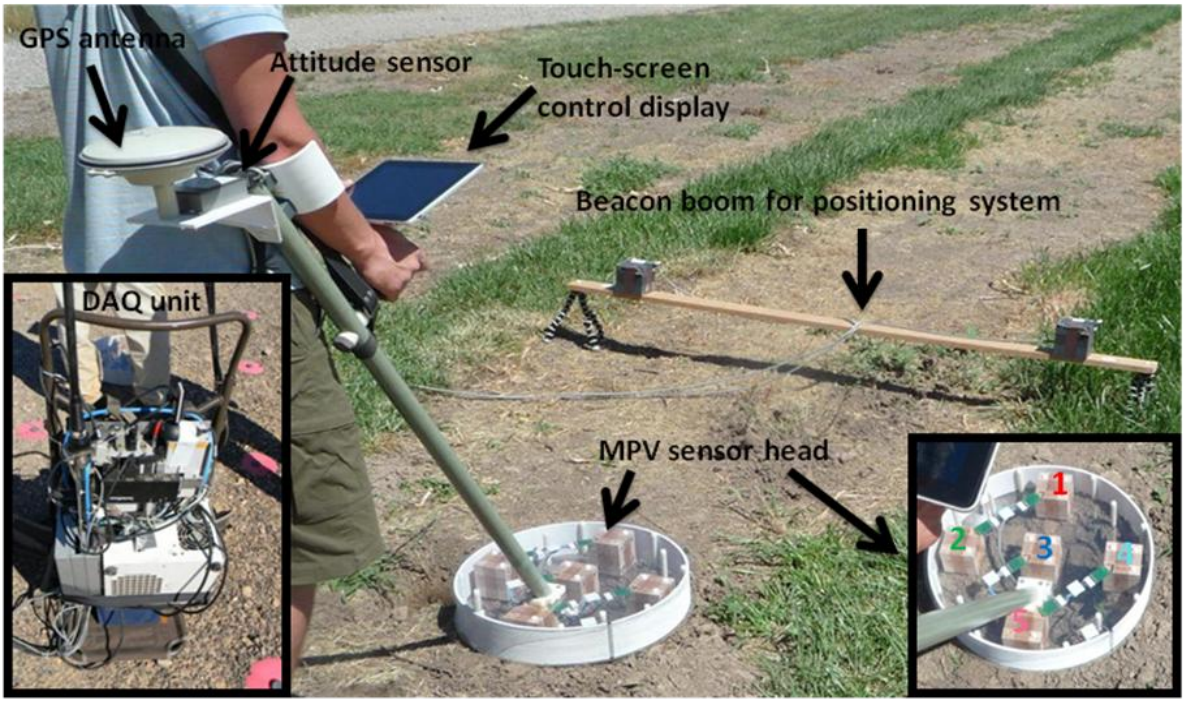

Figure 1: The second generation MPV with GPS (for open field survey) and beacon boom (for survey in forest, steep terrain). Left inset shows data acquisition (DAQ) and power unit mounted on a backpack frame.

A field survey with the MPV is performed with two complementary positioning systems. Detection mapping has minimal accuracy requirements and can be performed with a GPS, which could occasionally have a degraded signal without significantly affecting the survey quality. Discrimination through inversion of geophysical data requires accurate positioning of the sensor (Bell, 2005) and will be performed with a portable local positioning system. The operating principle consists of locating the origin of the primary field generated by the MPV transmitter coil, acting as a beacon, with a pair of EMI receivers rigidly attached to a portable beam, placed horizontally on the ground and supported by a pair of tripods to act as base station. The GPS will also be used to locate the beam in global coordinates for comparison with the geo-referenced ground truth locations. Field trials performed with the new MPV sensor head showed that the beacon system could predict MPV position and orientation relative to the beacon boom with an average accuracy of 1 cm and 1 degree, respectively, out to distances of 4 m. The combined MPV-beacon technology could facilitate advanced discrimination to any man-trafficable environments, in particular sites were traditional line-of-sight-based methods fail (e.g., at densely forested sites).

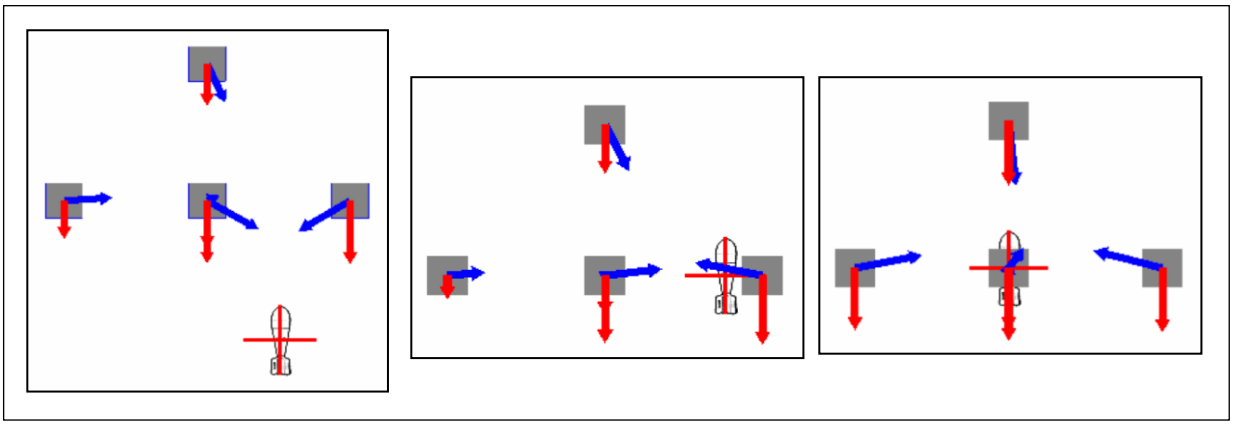

Figure 2: The MPV detection display window in dynamic data collection mode. The MPV user interface indicates with arrows the direction of the nearest compact metallic object relative to the MPV receiver cubes and directs the operator to the target, from detection (left panel) to location of that target (right panel).

2.2 MPV TECHNOLOGY DEVELOPMENT

Development and characterization of the MPV sensor were conducted under SERDP MM-1443 by ERDC-CRREL in Dartmouth, NH from 2005-2009 under the leadership of Benjamin Barrowes and Kevin O'Neil. The first MPV prototype was built in 2005-2006 by David George of G&G Sciences, Grand Junction, Colorado (CO). It was tested in 2007 at ERDC in a laboratory setting, where data were collected over a series of test ordnance in a highly controlled, low-noise environment. Interpretation of these data proved that the MPV could meet discrimination expectations under cooperative survey conditions (Figure 3 and Barrowes et al., 2007a, 2007b; Shubitidze et al., 2008). The ArcSecond laser positioning system was tested in 2007 and proved to deliver accurate location for local survey. The ArcSecond relied on three roaming laser stations and three receiver units placed on top of the MPV head.

The SERDP project was extended in 2008 to continue sensor testing and development of data modeling methods. The sensor was deployed in preliminary field tests at the Sky Research (SKY) test plot in Ashland, Oregon (OR) in the summer. A series of standard UXO were surveyed in various modes, static and dynamic, while location was provided using a template with marked locations and the ArcSecond. The effect of strongly magnetic soil on EMI sensors was also investigated during that survey as part of SERDP MM-1573 (PI: Len Pasion, Sky Research). The MPV offers possibilities to defeat that effect owing to its array structure (see Benefits section). Cued interrogation data provided stable discrimination results and confirmed the potential to extend advanced UXO classification capabilities to man-portable systems with the MPV.

These field tests also proved that positioning with ArcSecond was impractical and not reliable enough for effective field application because of the requirement to keep all three rovers in the field of view, and the long setup and calibration time. This experience led to development and testing of an alternative positioning method based on the beacon principle.

The SERDP project was extended in 2009 to test that beacon concept and prepare modification of the original MPV prototype for further field deployment. The sensor head was

redesigned and rebuilt in the Spring of 2010: lighter materials were employed and the circular head diameter was reduced to reduce weight and improve maneuverability, receiver cubes were brought inside the transmitter coil to reduce fragility, and transparent material was employed to allow the operator to see the ground through the unit. Figure 4 shows the first and second generation sensor heads for comparison. Detailed analysis of the sensor redesign is presented in Appendix D.

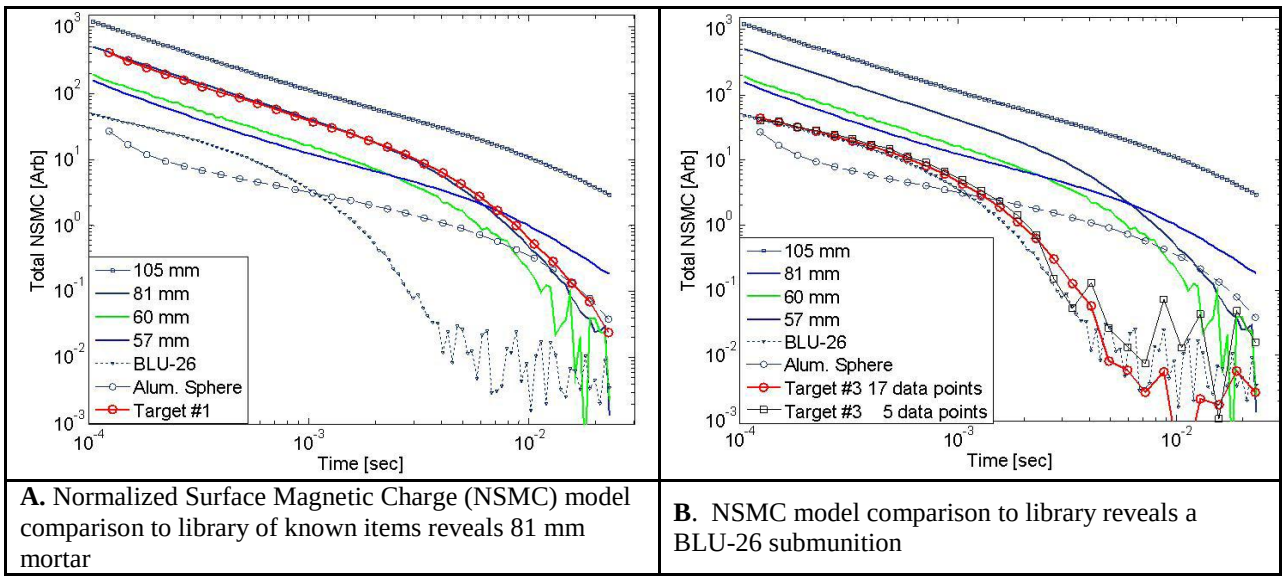

A. Normalized Surface Magnetic Charge (NSMC) model comparison to library of known items reveals 81 mm mortar

B. NSMC model comparison to library reveals a BLU-26 submunition

Figure 3: Classification result after inversion of MPV test-stand data with NSMC model. Inverted total charge is compared to a library of known items (blind test).

Figure 4: MPV prototype development. Right: original sensor (head weights 23 lbs). Left: second generation sensor with touch-screen control display (head weights 12 lbs).

2.3 ADVANTAGES AND LIMITATIONS OF THE MPV TECHNOLOGY

The MPV is the only available non-cart-based system that can acquire multi-static, multi-component data on a wide and programmable range of time channels.
The MPV offers several key benefits:

- By being man-portable, the MPV can be deployed at sites where terrain and vegetation preclude use of heavier, cart-based systems. The greater portability (no wheels) can greatly improve productivity, especially over rough terrain or for cued interrogation. Maneuverability also offers the ability to tilt the sensor head such that the transmitter illuminates the buried target at multiple angles. Standard horizontal loop transmitters produce a strong vertical field when directly above the target, with horizontal field components being significant when the transmitter is positioned at a standoff distance away. At these standoff distances, the magnitude of the transmit fields is reduced and lower signal-to-noise ratio data is acquired. By tilting the MPV we can take multiple "looks" of the target so that different combinations of the target's polarization tensor components are excited, resulting in more robust estimates of the target parameters and, therefore, more reliable discrimination (Smith et al., 2005).
- For each measurement, there are 5 receivers simultaneously recording three orthogonal components of the scattered field with near-perfect relative positioning among receivers. The multi-component, multi-axis design relaxes requirements on the number of soundings required to accurately predict depth, orientation, and target parameters, and on the positional accuracy (Grzegorczyk et al., 2009). This number of soundings is dependent on the target type and on field conditions. Processing of low-noise test-stand MPV data with perfect positioning has shown that a UXO can be identified with as few as 5 soundings (Barrowes et al., 2007b). Analysis of MPV data collected on the SKY UXO test plot in Ashland, OR over magnetic soil also show that a 4x4 grid of measurements could be used to robustly recover target parameters.
- The combination of multi-component and multi-time channel measurement capabilities and the geometric arrangement of the receivers offer potential for identifying and neutralizing the effect of magnetic soil, in particular with soil compensation techniques developed in SERDP MM-1414 and 1573. When the MPV is positioned with its sensor head parallel to ground surface, above magnetic soil over even ground (in the absence of a metallic target), signal in the receivers measuring the radial component of the signal (i.e., X component of side receivers and Y component of front receiver) should be equal, and the horizontal components of the co-axial receivers should be zero. The measured decays should have the characteristic decay of viscous remanent magnetic soil (Figure 5). The effect of soil can therefore be modeled and successful discrimination can be achieved even in the presence of magnetic soils (Lhomme et al., 2008; Pasion et al., 2008). The MPV response due to sensor motion and topography over magnetic soil is predicable (Kingdon et al., 2009). Soil characterization can also help exploit data collected when tilting the MPV to get multiple looks at an anomaly. These data would otherwise be difficult to interpret in presence of a significant background because the intensity of its effect would significantly vary between receivers. The ability to accurately model the MPV signal from compact metallic targets in the presence of magnetic soils is a key contributor to a robust inversion and discrimination capability.

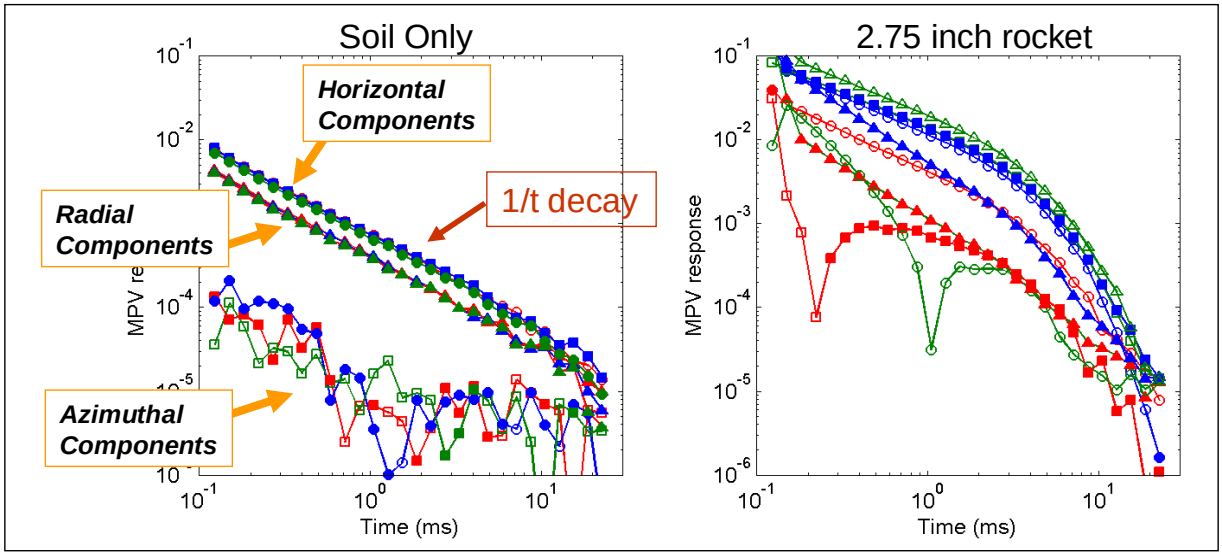

Figure 5: Comparison of MPV response between magnetic soil and a metallic target. Data collected at Sky Research test plot in Ashland, OR, where magnetic soils have shown to have a significant effect on EMI sensors (Pasion et al., 2008). The recorded signal (left panel) shows a time decay that is typical of soils with viscous remanent magnetization.

- The MPV is fully programmable and equipped with a graphical field-user interface that controls acquisition parameters such as transmitter waveform characteristics, the duration of the excitation, the number of measurement cycles to be stacked and the recording time channels. Short acquisition times are sufficient for detection, whereas discrimination improves with stacking many measurements over a long time window.
- The MPV has highly stable EMI components, which have a response that is directly predictable using standard EMI theory. In field tests conducted throughout all seasons of last year we verified that MPV components had imperceptible measurement drift and were largely insensitive to survey conditions (sun exposure, temperature). In general, instrument drift is removed by performing along-line high-pass filtering of the data, which has the potential of introducing filtering artifacts to the data and can bias target parameter estimates. A second method for identifying and removing instrument drift is to periodically measure the instrument response over a known item - this check is part of standard survey procedures performed in the field. The transmitter current is also monitored and recorded at all times during the survey to detect any variation in the excitation (e.g., due to changes in battery power).
- The MPV is well suited for small target discrimination. Smaller caliber anomalies have localized and rapidly-varying spatial response. An air induction coil measures a voltage by spatially averaging the secondary field of a target over the face of the loop. Therefore, large receivers tend to "smear out" the secondary field. The 8 cm x 8 cm receivers of the MPV are typically smaller than most multi-channel sensors (for example the Geonics EM63 receivers are 50x50 cm, TEMTADS are 25x25 cm) and thus better suited to detecting and sampling the secondary field over small targets.

3.0 PERFORMANCE OBJECTIVES

The performance objectives and results for this demonstration are summarized in Table 1. Results are mostly derived from the scoring report made by the Institute for Defense Analysis (IDA) and provided by Aberdeen Test Support Services. The report is included in Appendix B.

Success depends on the intrinsic quality of the MPV technology, on the quality of the survey protocol and implementation, and on the data analysis that ensues. Measured performance is a combination of these factors and accounts for the proposed one-pass survey protocol, which consists of covering the site in detection mode and interrupting momentarily the detection with a local cued interrogation survey (advanced characterization of an anomaly) whenever a detection threshold is exceeded. The main objective is to characterize the detection and characterization capability of the MPV as a function of the targets depth and size.

Table 1: Performance Objectives

Performance Objective	Metric	Data Required	Success Criteria	Results
Quantitative Performance Objectives				
Detection of all munitions of interest	Probability of detection (Pd) of seeded items at different depth	• List of potential targets • Rate of detection of seeded munitions	Pd>0.80 for all munitions in top 0.30 m and for medium and large munitions in top 1 m	Pd(z<0.3) = 1, Pd(0.3<z<1) = 0.90, with z the burial depth in meters
Minimize number of false detections (anomalies to investigate)	Number of targets selected for cued interrogation at a specified detection threshold	• List of detected targets • Probability of background alarm	Probability of false alarm (Pfa)<0.2 (no more than 1 in 5 detected items is non metallic)	Pfa = 0
Minimize number of anomalies to revisit	Rate of targets selected for cued interrogation after the initial survey	• List of detected targets and list of anomalies resurveyed	Less than 30% of anomalies need resurvey after initial survey	No anomaly was resurveyed
Maximize correct classification of munitions	Rate of munitions recommended for excavation	• Prioritized dig list with probabilities • Validation data for all selected targets	Probability of discrimination (Pdisc)> 0.80 for all munitions in top 0.30 m and for medium and large munitions in top 1 m	Pdisc(z<0.3)= 0.95 Pdisc(0.3<z<1) = 0.90
Reduction of false alarms for discrimination	Rate of false targets excavated before all targets are recovered	• Prioritized dig list with probabilities • Validation data for all selected targets	Leave at least 50% of clutter in the ground	Pfp(z<0.3) = 0.60 Pfp(0.3<z<1) = 0.75

Location accuracy	Average error and standard deviation in northing and easting for seeded munitions	• Location of seed items surveyed to 0.05 m accuracy • Estimated location from geophysical inversion	ΔN, ΔE and ΔZ <0.25 m	Mean ΔXY = 0.02 m Std ΔXY = 0.10 m Mean ΔZ = 0.01 m Std ΔZ = 0.09 m
Production rate	○ Acreage of field data or number of anomalies collected per day ○ Data analysis time / target	• Log of field work and data analysis time accurate to 15 minutes	• Survey: 0.5 acre per day or 100 anomalies • Mean analysis time: <5 minute per anomaly	Blind Grid: 400 anomalies were investigated in 4 days (26 h). Analysis time was greater than 5 min. per anomaly
Qualitative Performance Objectives				
Ease of use		• Feedback from technician on usability of technology and time required		Field technician was rapidly trained and found sensor to be easy to handle and survey with.

3.1 OBJECTIVE: DETECTION OF ALL MUNITIONS OF INTEREST

This is the primary objective of this demonstration. All shallow potential targets should be detected and recognized as such. Given that the MPV is a handheld-type EMI sensor, it is not expected to yield the same detection performance as large, wheel-based systems, which generate larger fields at depth and are able to detect deeply buried metallic bodies.

3.1.1 Metric

The metric for this objective is the number of detected targets as a function of the size and depth of the emplaced targets. The metric is conditioned by the scoring procedure applied at YPG, where three target sizes and three depth ranges are defined. Targets size ranges from small munitions type (caliber of ordnance smaller than 40 millimeters [mm]), to medium (40 to 81 mm caliber) and large (larger than 81 mm). Depth ranges are the top 0.30 m layer, then 0.30-1 m depth, and deeper than 1 m. Practically a continuous metric such as the Army's maximum detection depth of 11 ammunition diameter is inapplicable.

3.1.2 Data requirements

The demonstrator submitted a list of anomalies of interest with their location. The YPG administrators compared this list to the location of the seeded items and returned a detection rate by size and by depth.

3.1.3 Success criteria evaluation and results

The objective is met if the probability of detection (Pd) is 80% or greater for all munitions within the top 0.30 m, and 80% or greater for medium and large munitions in the top 1 m, assuming that small-caliber munitions are contained in the shallow top layer of the ground

(e.g., targets smaller than 60 mm should be in the top 0.5 m). Detection of deeper targets is considered as a bonus.

The probability of detection on the Blind Grid reaches 100% for all items within 0.30 m depth and 90% for items between 0.30-1 m depth, which satisfies the main detection objective for this man-portable sensor design (Appendix B, table 5). Deep targets remained below our detection threshold with a 0% detection rate on Blind Grid targets. This rate increases to 28% with the 90% upper confidence level on the probability of detection. In contrast, 155mm projectiles at 1.2 and 1.06 m were detected in the Calibration Lanes, while a 2.75 inch rocket at 1.2 m, 81mm at 1.5 m and 155mm at 1.5 m remained undetected. In terms of size, 95% of small, 75% of medium and 80% of large targets were detected. A discussion of the definition of target response is proposed in section 7.1. We anticipate that the detection performance would be similar with an alternative definition.

3.2 OBJECTIVE: MINIMIZE NUMBER OF FALSE DETECTIONS

Small coil receivers like those employed on the MPV are highly sensitive and have the potential caveat of detecting excessive surface clutter. One of the objectives of this demonstration is to minimize the number of anomalies of interest by limiting the number of false detections. Theoretically there is no surface clutter at the Standardized Test Site, but false alarms could still occur. The MPV user interface offers capabilities to identify false detections by displaying the signal amplitude and time decay on each receiver to help wean out odd or fast decaying anomalies. The operator was expected to perform this task in the field during the detection survey, thus saving the time of an additional cued interrogation survey. Detection data was also recorded and analyzed post survey, while at YPG, to control detection and potentially reassess detection thresholds and recommend suspicious targets for cued interrogation.

3.2.1 Metric

The metric for this objective is the number of anomalies selected for cued interrogation during the detection survey, augmented with eventual targets detected on the post-survey detection map.

3.2.2 Data requirements

The demonstrator supplied the list of anomalies of interest (anomalies selected for cued interrogation) for each area. YPG site evaluators compared the list to that of seeded items to obtain a false detection rate.

3.2.3 Success criteria evaluation and results

The objective is met if the number of detected targets surveyed in cued interrogations does not exceed the number of emplaced targets by more than 20% for the Blind Grid.

The objective was met as no false detection occurred. This optimal result was possible because the site had been well cleared of scrap and the EMI soil response is uniform and presents a weak magnetic effect.

3.3 OBJECTIVE: MINIMIZE NUMBER OF ANOMALIES TO REVISIT

Our survey protocol was based on collecting all the data necessary to characterize potential targets as part of the same survey. In contrast, existing advanced geophysical sensors (TEMTADS, MetalMapper) are generally deployed in cued interrogation mode to examine anomalies that were selected after analysis of a separate detection survey (e.g., with a Geonics EM-61, MetalMapper). This process can be slow, challenging and subject to errors as targets need to be geographically located and the sensor must be positioned such as to maximize the target response.

The MPV is equipped with real-time data feedback capabilities that allow the operator to visualize the measured data, assess data quality and identify potential targets while in the field. The objective is to take advantage of this capability to collect all the data necessary for characterizing a site without having to return to a given anomaly to collect additional data. Achieving this objective requires detecting all detectable anomalies during the dynamic search, and collecting sufficient data during a cued interrogation. The survey protocol is detailed in a later section.

One important point to note is that the detection phase was first verified in the field by taking a static shot over an empty cell, and later through mapping. This procedure is artificial and only applies to the Blind Grid, as potential targets are located at cell centers – this would not apply to a live site. If the static shot indicated the presence of a metallic object then the anomaly would be considered as a revisit. This confirmation shot provided data to assess the MPV detection capability with dynamic and static (higher SNR) data.

3.3.1 Metric

The metric for this objective is the number of anomalies that require additional data to be collected after the main survey, either because the targets were not detected or because the cued interrogation data were expected to be improved with recollection.

3.3.2 Data requirements

The number of targets to revisit is compared to the number of seeded items.

3.3.3 Success criteria evaluation and results

The objective would be met if less than 30% of anomalies need resurvey.

All detectable anomalies were found during the dynamic survey and inversion of cued interrogation data would not be improved with additional soundings. No resurvey was necessary, therefore objective was met.

3.4 OBJECTIVE: MAXIMIZE CORRECT CLASSIFICATION OF MUNITIONS

This is the second most important objective of the demonstration: all shallow munitions should be recommended for excavation after geophysical inversion. This objective requires that sufficient, high-quality data are collected, and that the ensuing data analysis, inversion and statistical classification process recognizes the presence of munitions. Our dig list also indicates our estimate of the target type.

3.4.1 Metric

The metric for this objective is the rate of munitions recommended for excavation.

3.4.2 Data requirements

The demonstrator submitted a priority dig list with the location of all potential munitions for evaluation. In return the evaluator scored as a function of munitions size class and depth range.

3.4.3 Success criteria evaluation and results

The objective is met if 80% of the munitions buried in the top 0.30 m are recommended for excavation, and 80% of the medium and large munitions down to 1 m depth.

Scoring was provided by depth or size. Results indicate that 95% of munitions within 0.30 m of the surface and 90% of munitions between 0.3-1 m were selected as targets of interest. Detection and discrimination rates roughly coincide, suggesting that most detected munitions were recognized as munitions during the discrimination analysis. This result is a success for the MPV technology and the classification method.

3.5 OBJECTIVE: REDUCTION OF FALSE ALARMS FOR DISCRIMINATION

This objective is related to the previous one. In general the result of classification is a priority dig list where targets are ranked according to their probability of being ordnance. The first items on the list are the anomalies for which the data do not support a rule-based decision (so called "can't analyze"). The list stops with the least likely potential ammunition. An efficient dig list would contain a minimum of non-hazardous targets. At YPG the demonstrator was expected to provide the probability of ordnance for each potential target location (grid cell centers).

3.5.1 Metric

The metric for this objective is the ratio of the number of non-ammunition items that were classified as UXO and the number of seeded non-ammunition items.

3.5.2 Data requirements

The demonstrator provided the probability of being ordnance for all potential target locations on the Blind Grid. The probabilities were compared to the ground truth by IDA.

3.5.3 Success criteria evaluation and results

The objective will be met if at least 50% of the clutter is left in the ground.

This objective was not completely met as 60% of the clutter in the top 0.30 m of soil and 75% of the clutter between 0.30-1.0 m were selected as targets of interest. The stated objective was too ambitious when considering the complexity of operating classification to identify 14 different types of munitions, and the fact that statistics are biased relative to a live demonstration where the number of scrap items is generally orders of magnitude larger than the number of buried munitions.

3.6 OBJECTIVE: LOCATION ACCURACY

Precisely locating targets of interest is essential for safe and efficient live site remediation. The combination of geo-location method and geophysical inversion should provide accurate guidance for safe and efficient target excavation. Achieving this objective would require accurate GPS referencing of the beacon boom that is used for locating the MPV during the cued interrogation, and accurate inference of the MPV location in beacon mode.

Note that results were only submitted for the Blind Grid, where targets are buried approximately at the cell center. Therefore only predicted depth could be scored by the evaluator. However, the predicted horizontal location can be compared to the cell-center location, assuming that targets were cell-centered. Location accuracy was also evaluated on the Calibration Lanes.

3.6.1 Metric

The metric for this objective is the horizontal and the vertical distance between the predicted and observed location of the munitions.

3.6.2 Data requirements

The demonstrator provided the predicted depth of the recommended munitions. The evaluator supplied the mean and standard deviation difference between the actual and predicted burial depth. Inversion results also provide

3.6.3 Success criteria evaluation and results

The objective would be met if the horizontal and vertical distance between the predicted and observed location was less than 0.25 m.

Results are presented in details in section 7.5. The objective is attained for the Calibration Lanes and the Blind Grid with mean horizontal and vertical offsets of less than 0.02 m and standard deviation less than 0.09 m.

3.7 OBJECTIVE: PRODUCTION RATE

The objective of the proposed survey protocol is to fully assess the ordnance contamination of a site in the minimum amount of time. Therefore cued interrogation is immediately performed when a potential target is detected to avoid the time-consuming task of relocating a target and bringing a geophysical sensor after an initial wide area detection survey.

3.7.1 Metric

The metrics for this objective are the daily rate of surveyed area, the daily rate of cued interrogations, and the average post-processing, data-analysis time per target. The first two rates depend on the ammunition contamination density.

3.7.2 Data requirements

The demonstrator tracked daily acreage surveyed, number of cued interrogations, and data analysis time.

3.7.3 Success criteria evaluation and results

The objective was to be met if, on average, every day the demonstrators were able to survey at least 0.5 acre or 100 anomalies (assuming 7 hours of effective survey, excepting the calibration lanes), and if the average analysis time was less than 5 minutes per target.

The summary of daily activities presented in section 7.6 shows that the survey rate on the blind grid is equivalent to 100 cued interrogations of anomalies per day. The acreage survey rate is not considered given the high target density. Data analysis processes were still at an experimental stage for the demonstration. The data were essentially new and therefore it took extra-time for the operator to become familiar with data features and data quality appraisal, to devise an appropriate geophysical inversion method and to formulate a suitable classification strategy. Additionally, development of analytical tools and programming was performed in conjunction with target analysis. Therefore the data analysis production rate was slower that it should be for a mature system. Faster analysis is expected for the upcoming Camp Beale Discrimination Study and in general for live-site demonstrations.

3.8 OBJECTIVE: EASE OF USE

The MPV is a prototype, advanced geophysical sensor that is not yet ready for commercialization, and therefore, might require special training. A series of data feedback features are incorporated in the field display user interface to guide the operator during data collection. Through critical evaluation by the experts (manufacturer, project manager) and training of a non-MPV-expert field operator we tried to assess the ease of use of the MPV. The geolocation procedure, which involves carrying a GPS for detection and registering the beacon boom with that GPS for cued interrogation, was also evaluated.

3.8.1 Qualitative criteria

The MPV was assessed for its physical requirements such as maneuverability, for the quality of its user interface in terms of ease of operation and usefulness of data feedback, and for the practicality of the positioning procedure.

3.8.2 Data requirements

A field geophysicist was trained on site to run a detection-discrimination survey with the MPV and later provided qualitative feedback on the sensor.

3.8.3 Success criteria evaluation and results

The objective was met if the trained field geophysicist could operate the MPV after two days of coaching without supervision.

The field geophysicist was able to operate the MPV in the field in less than a day and found the sensor to be reasonably straightforward to handle. In practice, the demonstration was performed with the Principal Investigator (PI) and the field geophysicist alternatively taking the "lead role", which consists in carrying the survey while holding the MPV and monitoring the sensor display to identify possible targets and decide on the number and location of cued interrogation soundings. Limited intervention or advice from the PI was necessary after the first day of survey.

4.0 SITE DESCRIPTION

The demonstration was performed at the Standardized Test Site at YPG, AZ. The test site was established as part of a multi-agency effort to provide test locations representing varied site terrain, geology, vegetative cover, and weather conditions that allows users and developers to define the range of applicability of specific UXO technologies, gather data on sensor and system performance, compare results, and document realistic cost and performance information.

4.1 SITE SELECTION

The YPG site was selected over the Aberdeen Proving Ground (APG) test site because of the timing of the demonstration (the desert presents less risk of rain or snow in the fall or winter, which could damage electronics and interrupt survey activities) and the occurrence of mild magnetic soil effects in some areas at YPG, which could bring further challenge and stimulate development of soil compensation methods.

The MPV was deployed at the Calibration Lanes to verify the survey method efficiency. The demonstration then proceeded to the Blind Grid and covered parts of the Desert Extreme sector in the open field area (Table 2).

4.2 SITE HISTORY

The YPG site is located adjacent to the Colorado River in the Sonoran Desert. The UXO Standardized Test Site is located south of Pole Line Road and east of the Countermine Testing and Training Range. The open field range, calibration grid, blind test grid, mogul area, and desert extreme area comprise the 350 m by 500 m general test site area. The open field site is the largest of the test sites and measures approximately 200 m by 350 m. To the east of the open field range are the calibration and blind test grids that measure 30 m by 40 m and 40 m by 40 m, respectively. South of the open field is the 135 m by 80 m mogul area consisting of a sequence of man-made depressions. The desert extreme area is located south east of the open field site and has dimensions of 50 m by 100 m. The desert extreme area, covered with desert-type vegetation, is used to test the performance of different sensor platforms in a more severe desert conditions/environment. Additional information about the site can be found at:

http://aec.army.mil/usaec/technology/uxo01c02.html.

4.3 SITE GEOLOGY

Refer to the YPG test site information provided at the website listed above.

4.4 MUNITIONS CONTAMINATION

Munitions present at the calibration lanes and test areas are described in Table 2.

Table 2: Layout Descriptions (http://aec.army.mil/usaec/technology/uxo01c02.html)

Test Area	Description
Calibration Lanes 0.27 acres	The calibration portion of the test site consists of at least nineteen (19) lanes. Seventeen (17) lanes contain six identical munitions buried in various orientations and at three different depths. One lane contains four (4) steel

Test Area	Description
	spheres buried at a depth of 0.5 to 2 meters. Another lane contains two (2) each (30.48 cm and 60.96 cm diameter) circular steel plates buried at 30.48 cm and 91.44 cm respectively. A third lane contains 15 cm and 30 cm diameter copper wire hoops (12, 16, 18 and 20 gauge) buried at 0.3 meters depth. The wire hoop gives a standard signature to compare to the signature the detection instrument is receiving. If an installation has site-specific munitions that are not part of the Standardized Target, extra calibration lanes can be added. Munitions generally rectangular in shape (aspect ratio not equal to one) are placed into the ground in six (6) orientations and at three (3) different depths. Munitions generally round in shape (aspect ratio of one) are buried at three different depths. The first and last opportunity of each Calibration Lane contains a 3.6 kg steel ball (diameter = 8.9cm) buried at 15 cm to provide a uniform signature that can be identified when looking at raw data.
Blind Test Grid 0.43 acres	The YPG Blind Test Grid (BTG) consists of a 1600 square meter area that is located east of the open field range. The BTG will be made up of the same type of munitions found in the Calibration Lanes and Open Field Site. Clutter items may include metal debris, rocks, desert vegetation roots, etc.
Desert Extreme 1.23 acres	The desert extreme portion of the test site consists of a 5,000 square meter area that is located south east of the open field site. The area is covered with desert-type vegetation and is used to test the performance of different sensor platforms in a more severe desert conditions/environment. The soils in this region may have a horizon of calcium carbonates that tend to cement together in the soil, producing hard layers in the subsurface. Ground temperature can reach up to 160 degrees Fahrenheit by early afternoon. Spring time air temperatures in shaded areas can exceed 110 degrees Fahrenheit.

5.0 TEST DESIGN

The goal of the demonstration is to prove the capability to detect shallow potential munitions and acquire the necessary data to classify detected targets with the MPV. The detection and discrimination performance of the sensor are characterized as a function of the size and depth of the buried targets and the presence and effect of aggravating factors (nearby object, magnetic soil and complex terrain).

5.1 CONCEPTUAL EXPERIMENTAL DESIGN

The experimental setup is reported in Table 3. The demonstration began at the calibration lanes, where the sensor was tested against a wide variety of items that are buried at different depths and orientations and for which ground truth is available. Sensor performance was immediately reviewed and compared with expectations in terms of target detection rate, of data quality and the efficiency of the one-pass detection-discrimination survey protocol. The sensor performance was deemed to be satisfactory. The demonstration proceeded to the blind grids and open field areas, where data were collected similar to a live site remediation project. Data quality control was performed both in the field and in the office, whereas the core of data analysis, inversion and classification, was executed after the field deployment. The original plan had the calibration taking place over days 1-2. It took one extra day to complete that stage.

Table 3: Demonstration steps

	Calibration Steps: Days 1-3				**Blind Grid and Open Field – Day Number**			
Tasks	**1.1**	**1.2**	**2-3**	**Off site**	**3 - 7**	**8 - 9**	**9**	**10 +**
Mobilization – Demobilization	X							X
CALIBRATION SURVEY: detection + discrimination		X						
CALIBRATION : DETECTION CHECK: 1. Detectability: signal amplitude as a function of target depth, size and orientation			X	X				
CALIBRATION : DETECTION CHECK: 2. Operational detection threshold: signal amplitude, detection rule, spatial coverage			X	X				
CALIBRATION : DETECTION CHECK: 3. Evaluation: too many/few detections?			X	X				
CALIBRATION : DISCRIMINATION CHECK: 1. Assess data quality as a function of target depth, size and orientation				X				
CALIBRATION : DISCRIMINATION CHECK 2. Classification: invert data and assess stability of recovered target parameters				X				
BLIND GRID SURVEY: detection + discrimination					X			

Tasks	Calibration Steps: Days 1-3				Blind Grid and Open Field – Day Number			
	1.1	1.2	2-3	Off site	3 - 7	8 - 9	9	10 +
DESERT EXTREME AREA: detection+discrimination						X		
Demobilization (packing)							X	
Data analysis: post YPG								X
Performance report: post YPG								X

5.2 SITE PREPARATION

There is no need for site preparation at YPG as it is a standardized test-site.

5.3 SYSTEM SPECIFICATION

The MPV was used in two distinct operating modes. During the detection survey, the system was set to dynamic acquisition mode, where short transmit-receive cycles are preferred because of sensor motion. Data blocks were 0.1 second (s) long with 2.6 ms time decay recording (9 repeats of 11.2 ms cycle). The signal was gated into 45 logarithmically spaced time channels.

For cued interrogation of a potential target, the system was set to static mode, where longer transmit-receive cycles and stacking are preferred to maximize data quality. The calibration area was surveyed with 8 ms time decay recording and stacking over 30 s periods with 50 time gates. Data quality and the stability of the recovered parameters were examined after the first day.

A Novatel Real-Time Kinematic (RTK) GPS operating at 20 Hertz (Hz) and an Applied Physics Systems 543 (high speed) attitude sensor were used for positioning and orienting the MPV during detection, and for registering the beacon boom location and orientation for cued interrogation (a regular sounding was taken at boom center). The azimuth reading was also used for cued interrogation because it cannot be recovered with the beacon since the MPV is circular.

5.4 CALIBRATION ACTIVITIES

As indicated in Table 3, testing at the calibration area was planned as a key procedure to ensure success for the rest of the demonstration. The field survey protocols used for the entire site were first tested at the calibration lanes by performing a one-pass, full-coverage detection survey which was momentarily interrupted every time a potential target was detected, so that a cued interrogation could be performed without having to relocate the target. Cued interrogation data were collected by taking static measurements over an imaginary grid centered on the peak anomaly, in addition to tilted measurements above the target. The MPV head was slanted at 45 degrees to vary the direction of the primary field relative to the target main axes while keeping a short standoff; this process improves the target geometric characterization. Cued interrogation data were processed and inverted to recover target location and parameters used for classification. Dipole model and surface magnetic source models were applied to try to obtain the best possible target classification result for the MPV.

The calibration lanes are organized such that depth of investigation and minimum detectable target size are directly measurable. Standard targets ranging from 20 mm to 155 mm projectiles are buried at various orientations and at three different depths, between 0.15 - 2 m.

The key objectives are listed below.

For detection:

- To validate the dynamic mode data acquisition parameters by verifying that all targets are detected;
- To validate the detection survey protocol and verify full coverage by generating a digital detection map (post survey);
- To define detection thresholds to minimize the number of anomalies to interrogate (reject small clutter and avoid false detections);
- To determine the maximum detection depth for different target sizes, and to assess the effect of complicating factors (e.g., nearby clutter, if applicable);
- To assess the efficiency and practicality of the proposed survey method (detection immediately followed with cued interrogation); and
- To evaluate the ease of use of the sensor and its user interface.

For cued interrogation and classification:

- To validate the static mode data acquisition parameters
- To test the practicality of the survey protocol with beacon boom for positioning
- To assess the quality of infield feedback on data quality
- To measure the effect of target depth and size on data quality and the recovery of target parameters for classification

Different data processing schemes were tested on the calibration data and compared with target ground truth:

- To assess the effect of the number and type of soundings on recovered parameters, which would help optimize data collection by minimizing the amount of non-informative or redundant data
- To investigate potential differences in discrimination with dipole and magnetic source models.

5.5 DATA COLLECTION PROCEDURES

The geophysical data are comprised of EMI sensor and location measurements. Data were recorded during all phases of the deployment. The MPV data acquisition system (DAQ) handles and merges all sensor data and produces individual files (.csv) for each detection survey segment (between two consecutive cued interrogations) and each target.

Scale:

The goal is to fully characterize as much terrain as possible and achieve an average of 0.5 acre per day (detection and cued). The calibration lanes (0.3 acre) and blind grid (0.5 acre) were visited in priority before surveying other parts of the open field (map shown in Figure 6). The calibration

area (0.3 acres) results were not rated for productivity, as different survey protocols were tested and validated.

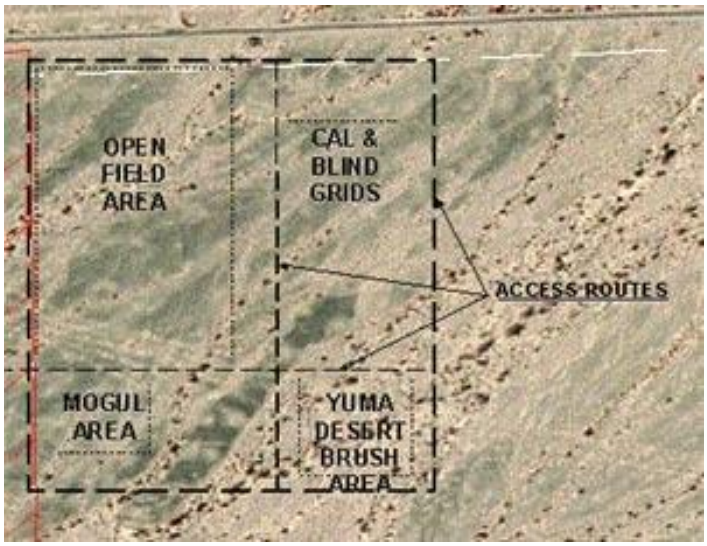

Figure 6: Map of YPG field sites.

Sample density:

Detection- the field operator walked along pre-programmed straight lines while sweeping the sensor head following an "S" pattern along track. The sensor head diameter is 0.5 m. Adopting 1-m cross-track spacing produces full coverage while sweeping with amplitude and period of 0.5-0.6 m. Given EMI and GPS data update rates of 10 Hz and receivers coil size of 0.08 m, it is preferable to keep the sensor head speed below 0.5 m/s. In that case the along-line survey speed would be about 0.2-0.3 m/s.

Cued interrogation: Successful target characterization relies on the capability to excite the different polarizability axes of the target and acquire high quality data (high signal to noise ratio). This requires varying the relative angle of the transmitter coil and target for the excitation, and keeping as close as possible to the target for the data collection. Different excitation directions are usually achieved in a flat survey when the transmitter is located to the side of the target, at the cost of signal amplitude. This conundrum is here resolved with a handheld sensor and a positioning devise that tracks the sensor orientation by tilting the MPV in different direction while staying in the vicinity of the expected target position. Receiver cube centers are separated by 0.2 m, whereas the transmitter coil is 0.5 m in diameter. We performed the cued interrogation in a star pattern with 0.5-m spacing with the MPV placed in horizontal position. Tilted measurements were also acquired directly over the estimated target position.

Quality checks:

- Detection was verified at multiple stages. During the detection survey, the dancing arrows display was calibrated to null the background response and would generally indicate the presence of a metallic object with most arrows growing in amplitude and pointing in the same direction. When a target would be detected, the operator would continue surveying the EMI signal over the entire cell to map the anomaly extent and identify potential secondary targets. The operator would return to the peak signal location – or between the two peaks when applicable – then stop the dynamic survey. The last recorded EMI amplitudes and decays would be displayed, thus

allowing the operator to make a guess on the target location and type. A second detection check was possible because potential targets were expected near cell centers. A static shot was taken at the cell center to confirm that that the operator did not miss a target. This also provided a mean to compare the SNR levels of dynamic and static data – there is a chance that a target would not appear in dynamic mode because the SNR is lower and because the arrows reflect the EMI response integrated over the entire time range. We never found that we had missed a target. A third control on detection can be done by producing a detection map – note that mapping and interpreting multi-component, multi-axis data is not straightforward.

- Spatial coverage was verified in two stages. The sensor track was displayed in real-time on the sensor control panel along with the pre-programmed lines so that gaps stand out. A digital geophysical map of the detection survey provided a second control.

- Error detection: Receiver malfunction or the presence of parasitic signal could be detected by displaying the recorded signal amplitude as a function of time each time the survey was interrupted. In terms of positioning, the MPV operating software, EM3D, accepts a National Marine Electronics Association GPS Fix Information (NMEA GGA) string from the GPS at 20 pulses per second (pps) for G&G Science's Novatel system, or at 10 pps for the Sky Trimble system used at Camp Butner. The string is parsed for its parameters, including the so-called Q-factor. In the GGA string, Q=4 is the RTK solution (2cm). EM3D monitors the Q factor and immediately displays an error screen any time that Q is not equal to 4.

- Cued interrogation: Dancing arrows were used to locate the target and maximize the chance of acquiring high SNR data. Quality of the EMI data was controlled by plotting the recorded signal for each receiver after each sounding. Quality of the beacon positioning was estimated by monitoring the signal amplitude of beacon cubes and the digital compass output.

Noise levels were documented by taking calibration measurements above a target-free area and end-of-line shotputs every time the sensor was switched on or off to verify lack of sensor drift. Periodic measurements of the intrinsic noise level (in air) and the background soil response were collected.

Data handling:

The MPV DAQ wrote binary files (.tem) that were locally converted to ASCII files (.csv) and saved to an external disc before switching the system off (e.g., battery change, end of day). Data were copied to external computers for archiving and post processing (MatLab, UXOLab).

5.6 VALIDATION

Validation was provided through the available ground truth at the calibration lanes, which provide means to control the ability to predict the location and depth of a target and the stability of the recovered target parameters. Similar munitions were expected throughout the YPG site. We assumed that all munitions types were present in the calibration lanes for training.

6.0 DATA ANALYSIS AND PRODUCTS

6.1 PREPROCESSING

Control of the transmitter and recording of the receivers' response was handled by the DAQ, which uses similar programs as the MetalMapper employed in previous ESTCP studies. Through the DAQ the receiver data streams were gated and stacked, then merged with the geolocation data and saved into binary and ASCII files for additional analysis.

The recorded EMI signal includes a background response from the sensor noise and the soil magnetization. The background response was measured during sensor checkups and soil response assessment tests to ensure that the response was spatially uniform across the site and stable with time (independent of battery condition). Analysis of the background response was performed in the MatLab computing environment after the field survey. Figure 7 shows static measurements of the in air response, which mostly contains the sensor noise, and the response above empty cells, which reveals soil magnetic effects. Each receiver has a distinct and repeatable signature; the Z-component response is stronger because of coupling both with the Transmitter coil and with the soil. After verification of the background response stability, the average response was computed for each receiver as a function of the time gate. Because the early time amplitude is particularly large, it could significantly contaminate the signal for weak target responses. Therefore static cued interrogation data had the background response removed before geophysical inversion.

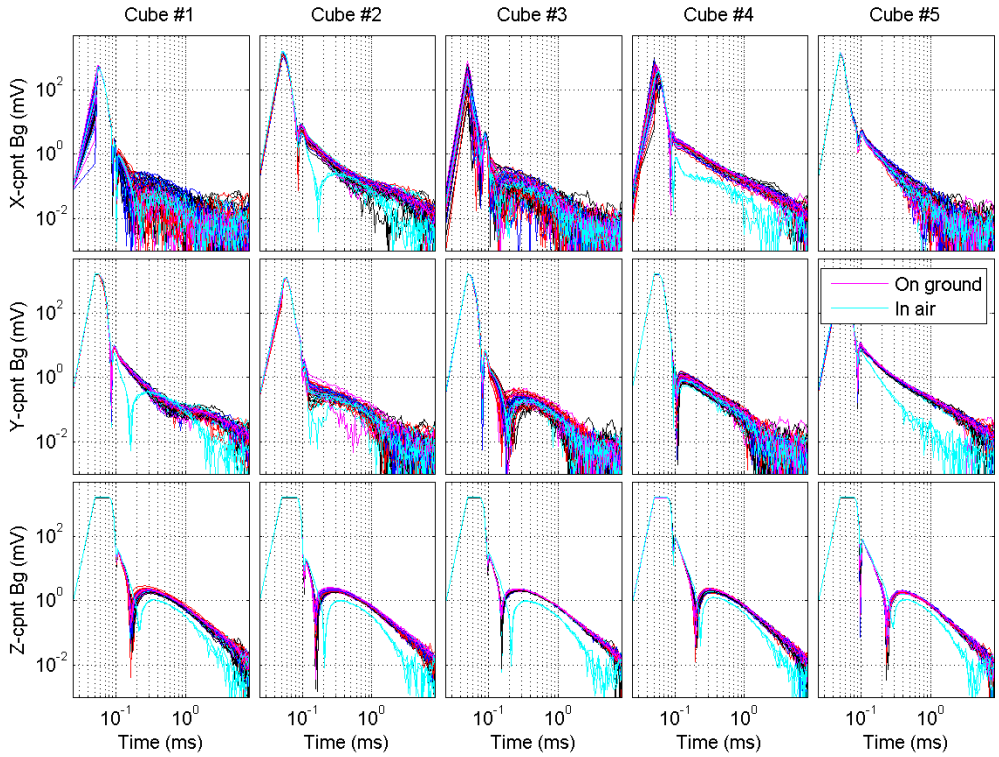

Figure 7: Background noise. EMI response when sensor is placed on the ground in the absence of any metallic targets, and response when held in air.

6.2 TARGET DETECTION

Target detection was performed in real time based on the MPV detection window (dancing arrows, signal amplitude and time decay) and verified after completion of data collection by generating a detection map. The calibration lanes were surveyed with an ad hoc detection thresholds based on data recently collected in Grand Junction, CO with the new sensor head. These thresholds defined the sensitivity of the arrows display and were set so that arrows would have high sensitivity to low amplitude signal using linear scaling, and a logarithmic scaling for larger amplitude to avoid saturating the window with large responses. The detection rule for the remainder of the survey (blind grid and open field) was defined after evaluation of the calibration lanes, where targets are located and identified. The detection data were analyzed at the end of each day to verify that all potential targets have been detected and sufficiently characterized.

6.3 PARAMETER ESTIMATION

Static data were merged on a cell by cell basis – there were 5-8 soundings plus one tilt test per anomaly – and analyzed to verify that there were no corrupt data, and then inverted using a dipole model or a surface magnetic source model.

Feature extraction with the dipole model

In the EMI method, a time varying field illuminates a buried, conductive target. This illuminating – or primary – field induces currents in the target that subsequently decay, generating a decaying secondary field that is measured at the surface. These data are then used to estimate the position, orientation, and parameters related to the target's material properties and shape. In the UXO community, it is commonly assumed that the secondary field can be accurately approximated as a point dipole (e.g., Bell et al. 2001, Pasion and Oldenburg 2001, Gasperikova et al. 2009). The process of estimating the parameters of the dipole forward model from the data is called data inversion.

The dipole model assumes that the time-varying secondary magnetic field $\mathbf{B}(t)$, is due to a point dipole $\mathbf{m}(t)$ located at $\mathbf{r}$:

$$\mathbf{B}(t) = \frac{\mu_o}{4\pi r^3}\mathbf{m}(t)\cdot\left(3\hat{\mathbf{r}}\hat{\mathbf{r}} - \bar{\bar{\mathbf{I}}}\right), \tag{1}$$

where $\hat{\mathbf{r}} = \mathbf{r}/|\mathbf{r}|$ is the unit-vector pointing from the dipole to the observation point, $\mathbf{I}$ is the 3 x 3 identity matrix, $\mu_o = 4\pi \times 10^{-7}$ H/m is the permittivity of free space and $r = |\mathbf{r}|$ is the distance between the center of the object and the observation point. The dipole induced by the interaction of the primary field $\mathbf{B}_o$ and the buried target is given by:

$$\mathbf{m}(t) = \frac{1}{\mu_o}\bar{\bar{\mathbf{M}}}(t)\cdot\mathbf{B}_o, \tag{2}$$

where $\mathbf{M}(t)$ is the target's polarizability tensor. The tensor reflects the characteristics of the buried target in terms of its shape, size, and material properties. It is written as:

$$\bar{\bar{\mathbf{M}}}(t) = \begin{bmatrix} L_1(t) & 0 & 0 \\ 0 & L_2(t) & 0 \\ 0 & 0 & L_3(t) \end{bmatrix} \tag{3}$$

The magnitude and decay of the polarizability tensor elements is a function of the size and electromagnetic properties of the target. The relative sizes of the tensor elements are indicative of the target shape. If ordering tensor elements such that $L_1>L_2>L_3$, then a steel body-of-revolution (BOR) would have $L_2=L_3$ for a rod-like object and $L_1=L_2$ for a plate-like object.

The target parameters of the dipole model (i.e. location, orientation, and polarizability tensor elements) are estimated in the process of data inversion. The objective of data inversion is to determine the set of parameters that most accurately predict the observed data. Numerical optimization methods are used to determine the parameters that minimize a data misfit objective function:

$$\textit{minimize} \quad \phi(\mathbf{m}) = \frac{1}{2} \| V_d^{-1/2} (d^{obs} - F(\mathbf{m}_{target})) \| \quad \textit{subject to} \quad m^{\inf} \le \mathbf{m}_{target} \le m^{\sup} \tag{4}$$

where F is the forward modelling operator and V_d is the data covariance matrix, which includes a user-defined noise estimate. The noise estimate corresponds to not explicitly modelled phenomena that can affect the data, such as sensor noise, geologic effects and positional error. We assume that noise is composed of a base level plus a factor that is proportional to the signal amplitude. In UXOLab noise parameters are set by the user before an inversion. The dipole model is an ideal candidate for inversion because (1) the forward model is physics based with parameters that tell us something about the characteristics of the target and (2) the forward model is fast to compute, which is important since numerical optimization can involve an extensive search of parameter space involving numerous calculations of the forward model.

Case of overlapping anomalies

At highly contaminated sites, anomalies will often overlap due to the close proximity of multiple targets. Our data inversion strategy for overlapping targets is to decompose the inverse problem into several steps. Each step resolves a subset of model parameters. The first step is to solve for non-linear location parameters and subsequently solve for linear polarization parameters. With an optimal estimate of locations and dipolar polarizations, the orientations of each object can be extracted from estimated magnetic polarizability tensors. For time-domain systems that have sufficient time channels to characterize the decay behavior of the polarizability, we further seek the set of parameters in a parametric model of dipolar polarizations by either fixing the locations and orientations of multiple objects derived in the two-step procedure, or incorporating these nonlinear parameters into the inversion for an update. Our multi-object inversion approach has been successfully tested as part of previous Discrimination Studies with ESTCP with Geonics EM63 data (Former Camp Sibert, Alabama) and with static MetalMapper data (San Luis Obispo, California).

Surface magnetic source models

The data also were inverted using normalized surface or volume magnetic source models (NSMS or NVMS) to characterize the EMI response from subsurface targets. The models distribute surface or volumetric dipole (or elementary charge) sources on or inside a spheroid assumed to envelope the assumed target. Different inversion approaches can find the collection of sources that best describes the observed data. This collection of sources has a higher resolution and exhibits a better fidelity for matching complex EMI responses from heterogeneous targets than a point dipole model. The surface or volume summation of these sources, the total NSMS (TNSMS) is invariant to the position and orientation of the target. The inversion process that obtains the TNSMS of the subsurface target also produces an estimate of the position of the

target. The rotation matrix that translates the reference frame of the target to the global reference frame is also extracted in the process so that both the position and orientation are estimated as well as the TNSMS. We use various algorithms such as differential evolution (DE) and simplex minimization to invert for the target parameters. When there is more than one target in the field of view of the sensor, either a two target NSMS algorithm is used or an ortho-normalized volumetric source approach is adopted.

6.4 TRAINING

The calibration lanes contain approximately 100 anomalies, including all munitions that can be encountered at the site and some clutter. Munitions are buried at various depths and orientations, thus providing the opportunity to adjust inversion noise estimates and measure the variance of the feature vectors.

Most anomalies were successfully inverted (Figure 8), resulting in correct depth predictions. Targets with low SNR because of their small size or great depth could not be inverted. For instance, the two 81 mm projectiles buried at 1.5 m were invisible in the EMI data. One 60 mm projectile buried at 0.40 cm depth in horizontal position also had low SNR and caused a failed inversion. Overall, the calibration lanes provided sufficient data to train for the blind grid test.

Classification is discussed in the following section. Features were derived from polarization tensor parameters (depth, polarizability eigenvalues, polarizability or NSMS decay rates), from data metrics (e.g., signal-to-noise ratio) and from inversion quality assessment (e.g., data misfit and correlation coefficient).

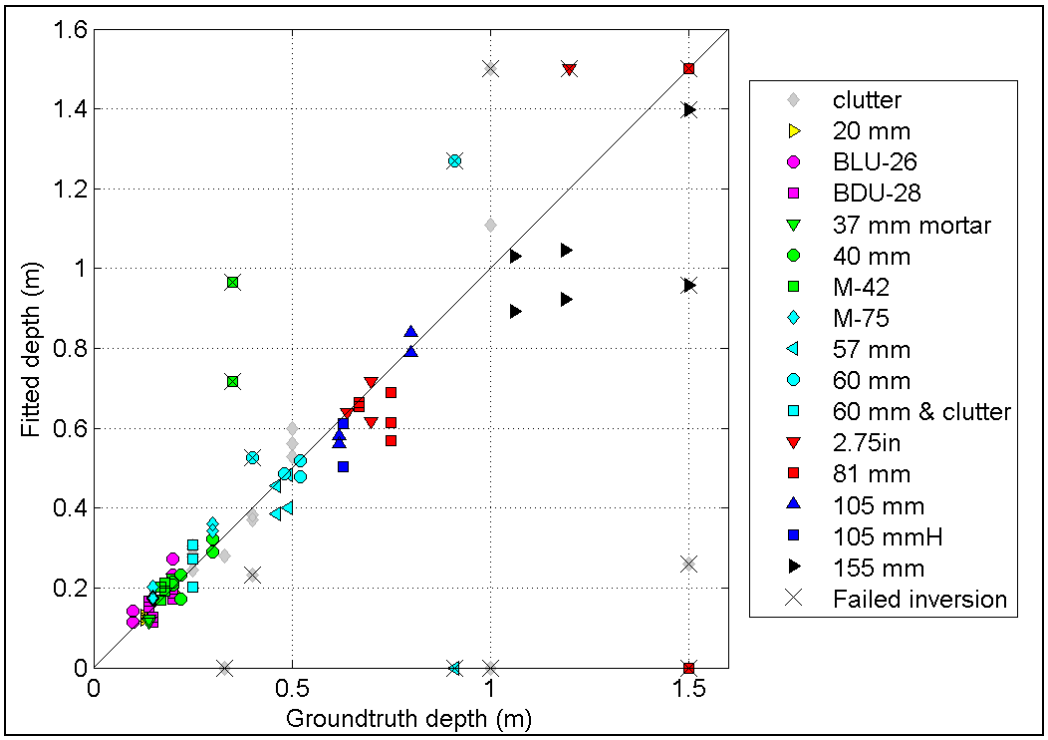

Figure 8: Seeded depth and predicted depth for YPG calibration lanes. Anomalies with low SNR had failed inversions.

6.5 CLASSIFICATION

Statistical classification: The following guiding principles were applied:

- *Selection of features:* By analysis of the training data, those features that contribute to separation of the different classes (comprising UXO types and clutter) are selected. This selection involves canonical analysis to determine the combinations of features that contribute most to class separation. Statistical testing is used to assess whether there is adequate separation between classes to justify using statistical classifiers.
- *Choice of classification algorithm:* Through analysis of the training data the best performing classifier (rule-based, support-vector-machine, probabilistic neural network, discriminant analysis) is selected.
- *Classification:* Anomalies are placed in a prioritized dig-list by using the classifier to compute probabilities of class membership for unlabeled feature vectors. The probability of membership of the clutter class is reported on the dig sheet.
- *Number of UXO-classes*: More than one UXO class is required at YPG as there are fourteen (14) different types of UXO with widely different size. When multiple UXO classes need to be used (assume there are M of them) then one can either train an (M+1)-class classifier, or train M two-class classifiers and combine the results.

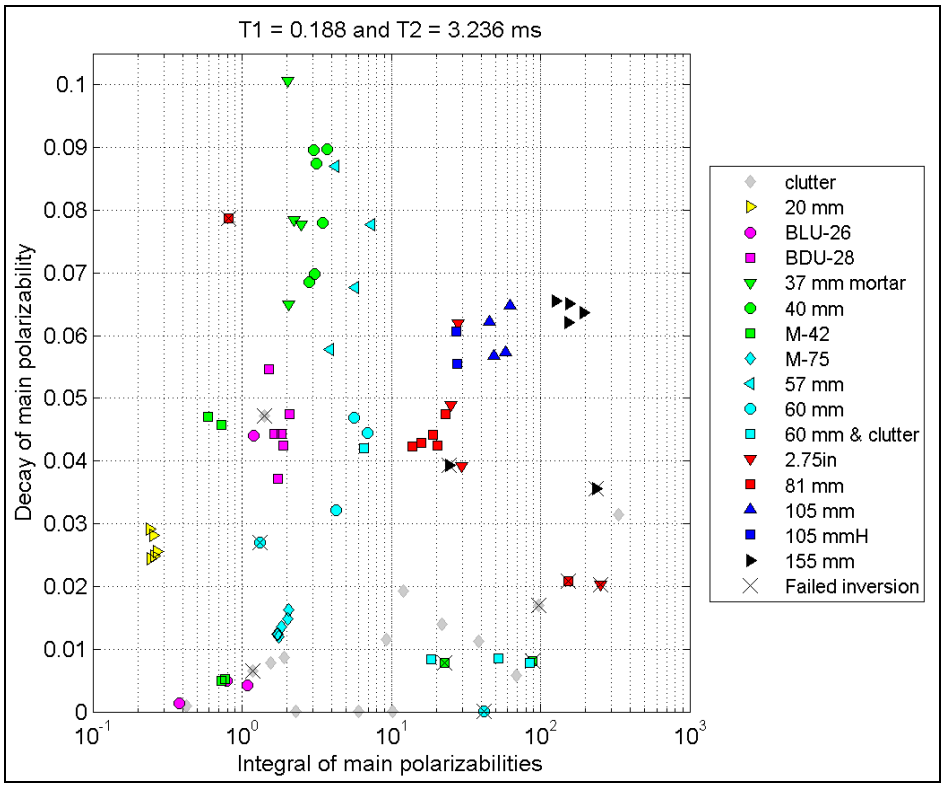

Figure 9: Size and time-based classification of training data. The size parameter is here chosen as the time integral of the three main polarizabilities. The time-based feature is chosen as the ratio of the principle polarizability (L1) at late time 3.236 ms and early time 0.188 ms. (Note: anomalies resulting from 60 mm projectile and clutter were here inverted as single targets to assess the adverse effect of a wrong diagnostic on classifiction. Inversion with multi-target algorithm yielded better result but its use was not warranted for success of this demonstration as no multi-target are expected on the blind grid.)

Generally, a classifier comprises a combination of a size and a time-based feature (as was used in SKY's previous demonstrations with ESTCP at San Luis Obispo, Camp Sibert and Fort McClellan). The definition of one or several munitions classes is here complicated with the presence of 14 munitions types spanning a wide range of physical properties and sizes, from 20 mm to 155 mm projectiles. The training data were also biased by containing mostly munitions (80% of the anomalies), as opposed to the somewhat balanced and representative samples of munitions and clutter encountered at previous demonstration studies. In anticipation with these potential challenges the final decision on the classifier were postponed till the training data had thoroughly been analyzed.

A size and time-based classifier is illustrated in Figure 9, where training targets from the calibration lanes are presented. As expected the wide range of munitions occupies a large portion of feature space with limited separation, and therefore limited capability for clutter differentiation. The classifier should include more features to take advantage the MPV data richness.

Library Based methods: Given the wide variety of target types and the small representation of training clutter, the definition of UXO classes and application of a statistical classifier would not necessarily provide sufficient separation between all munitions and clutter. Therefore we also considered classification with a library-based method using the same dipole model inversion results as for the statistical classifier. For each target type the feature vectors were the primary, secondary and tertiary polarizability time decay curves. A munitions library was constituted with the training data by considering all occurrence of a munitions type to define the reference polarizability decays and associated variability. Recovered polarizabilities for the calibration lanes are shown in Figure 10. Polarizabilities are remarkably stable for most munitions types, showing that each type has a specific signature in terms of amplitude and time decay rates and confirming the capability to recover the body-of-revolution characteristic (L2=L3).

Adopted classification strategy: Concurrent classification methods were applied:

- For library-based classification, the recovered polarizability decays of each unknown target were compared to those of library items. The probability of being a UXO was defined after computing the smallest difference with all library items, and normalizing to obtain a metric varying between 0 and 1. Note that the library based technique is particularly effective when (1) there is a good understanding of which UXO can be expected at the site, and (2) there are scrap targets that have a unique polarization tensor (for example, base-plates at calibration lanes).

- For statistical classification, feature vectors were comprised of the recovered polarizabilities for a subset of time channels. In order to favor the main polarizability, which is the most stable one, and utilize the discrimination potential of late time information, all channels were used for L1, whereas only early times were used for L2 and L3 to keep shape information. Choice of the number of classes is a tradeoff: when using few classes the capability to separate targets is diminished because different types of munitions are lumped in the same class; when using as many classes as there are munitions, there is a risk of being too aggressive if SNR is too low to allow recovery of stable polarizabilities, especially when considering that only 3-5 instances of each munitions type were available for training. We tested a Support-Vector-Machine (SVM) classifier with 4, 6 and 8 ordnance classes. Each class was trained against the remaining training munitions and clutter. The SVM algorithm used the MatLab-enabled Spyder toolbox, which was also Sky Research classifier of choice for the ESTCP Camp Butner demonstration (ESTCP-

201004). We chose to apply the 6-class classifier with separate classes for 155-105mm, 81mm-2.75", 60-57mm, 37-40mm, 20mm-M75-BDU28 and M42-BLU26.

- The final probability of UXO was taken as the maximum of the two here-above probabilities, and manually reviewed by a geophysicist. Probability of the most ambiguous targets was altered to obtain a just-above-threshold value.

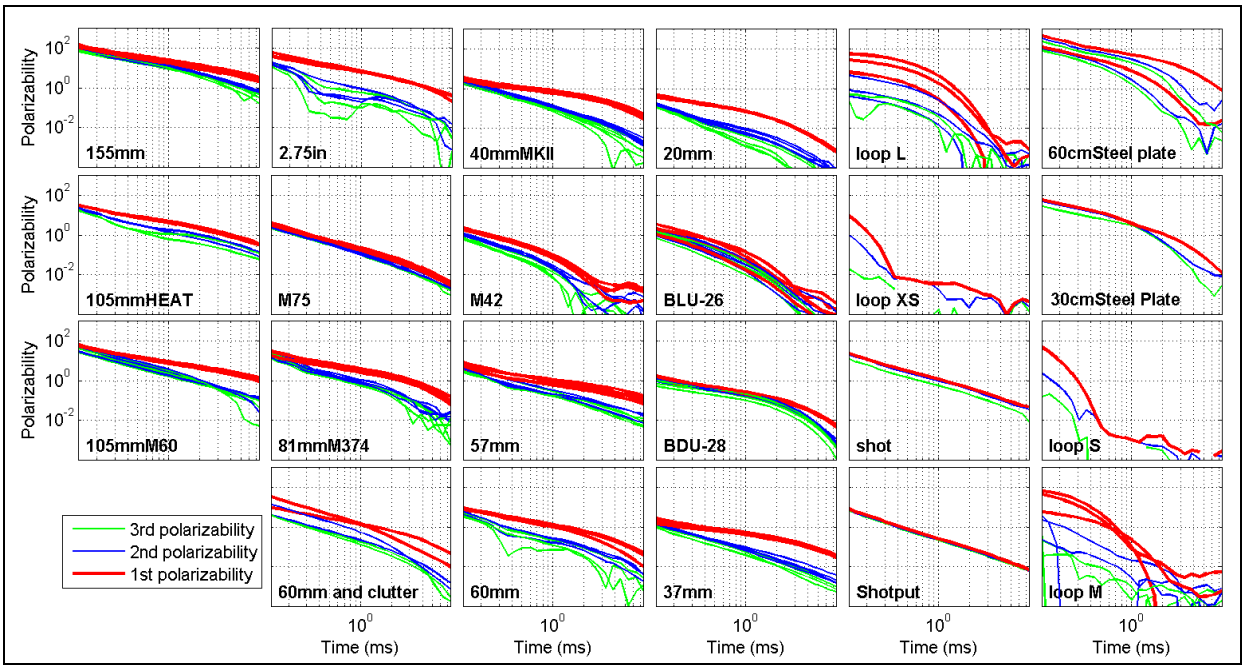

Figure 10: Recovered polarizabilities for successful inversion of training targets from calibration lanes. Main polarizability (L1) is showed in red; secondary polarizabilities (L2, L3) are showed in blue and green. For the 2.75" rocket, the two least stable results correspond to low SNR cases with the target buried at 0.70 m depth in vertical position, where second polrizabilities are more difficult to characterize.

6.6 DATA PRODUCT SPECIFICATION

Data were delivered to Aberdeen Test Center according to YPG test guidelines and consisted of:

- The collected geophysical data (merged EMI data and positioning data: GPS and digital compass); for the cued interrogation data we also supplied the recorded beacon data;
- Classification results: the list of potential target location with detection stage response, predict depth, probability of being UXO and an indication of the target-size class.

Data are also available to ESTCP and its partners. Additional data are presented in the performance analysis section of this document.

7.0 PERFORMANCE ASSESSMENT

This section presents an analysis of the demonstration performance, starting with the eight demonstration objectives and augmented with additional sensor performance topics.

7.1 OBJECTIVE: DETECTION OF ALL MUNITIONS OF INTEREST

The detection protocol was tested on the Calibration Grids. The operator surveyed each cell as if there was no *a priori* information about the presence of a target in the cell. Detection was based on the arrows display, which shows the direction and amplitude of the measured horizontal and vertical components of the scattered magnetic field integrated over the entire recorded time window. This method can wean out some of the small clutter because clutter – non-UXO items – have fast decay rate, therefore their late-time response is lesser than the noise level. The current incarnation of the MPV DAQ does not include a threshold-based alarm; the operator simply monitored the arrows during detection and confirmed detection with a static measurement on top of the expected anomaly location.

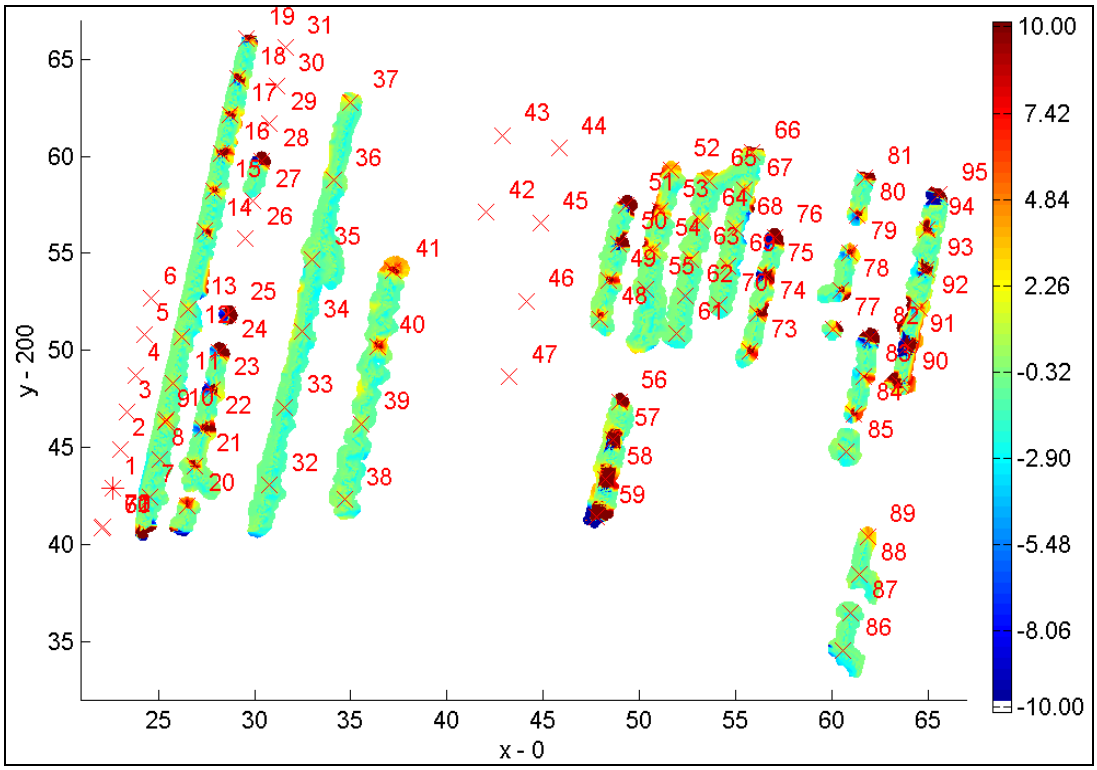

Figure 11: Detection map of Calibration Lanes using Z component data of central receiver. Targets are located with a cross marker; target number is indicated NE of target location.

A detection map of the Calibration Lanes is presented in Figure 11. The first line that contains targets 1-6 is omitted because the detection protocol was being tested with a short 0.9 ms excitation time – this is the usual setting for MetalMapper survey. Excitation time was subsequently increased to 2.6 ms to obtain a longer time window for inversion of dynamic data (see later discussion). Most targets appear clearly on the map. Targets 7-8 are invisible and

correspond to deep 81 mm mortars that could not be reliably inverted because even the cued interrogation data had too weak EMI response.

The definition of the target Response Stage (RS) for the submitted dig list was based on the amplitude of the target response in static mode for convenience at the time. The amplitude of the response was computed as mean square root (norm) of the target response measured on all 15 receivers at 0.16 ms. Alternative definitions could have been employed and would have yielded qualitatively similar results. The left panel of Figure 12 shows that the norm and the maximum amplitude among all receivers for all calibration targets are highly correlated; a target response including all receiver units had originally been chosen for clutter rejection, assuming that clutter would only appear on a small subset of the 15 receivers. The right panel of Figure 12 shows high correlation between the signal computed at early time and signal integrated over the entire time window for the calibration targets. The outliers are large targets with slow time decay, which suggests utilizing the integrated signal for detection. Figure 13 compares the raw – not-background corrected – dynamic and static responses, using the maximum recorded signal measured on a receiver. The static and dynamic responses are highly correlated at early time. Correlation is less pronounced with the time integrated responses because the integrating windows have different duration (2.6 and 8 ms) and decay rates vary between targets, but the general trend remains. Therefore the definition of RS adopted for the submitted dig list applies for dynamic detection data.

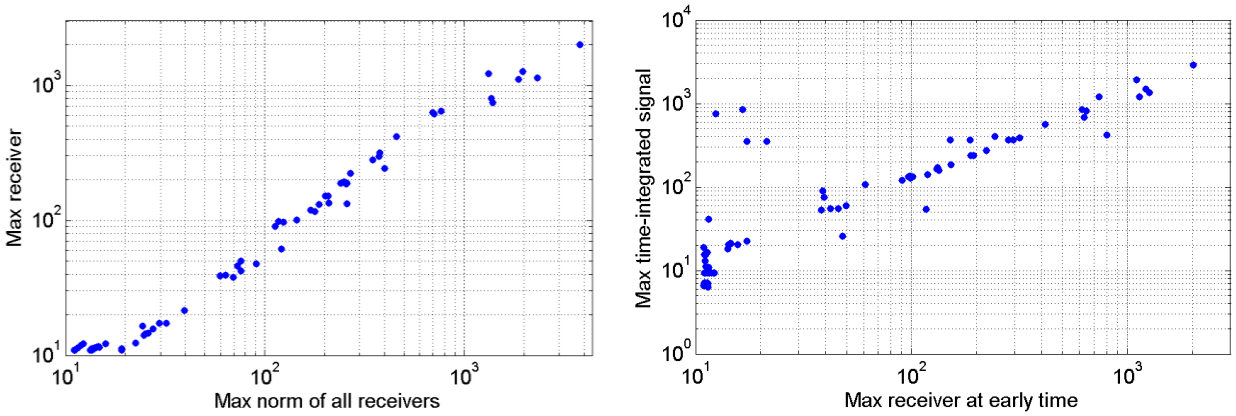

Figure 12: Analysis of target response stage with different definitions. Left: RS defined as maximum norm versus maximum amplitude recorded on a receiver. Right: RS computed on early time versus integrated over entire recorded time window, using maximum receiver.

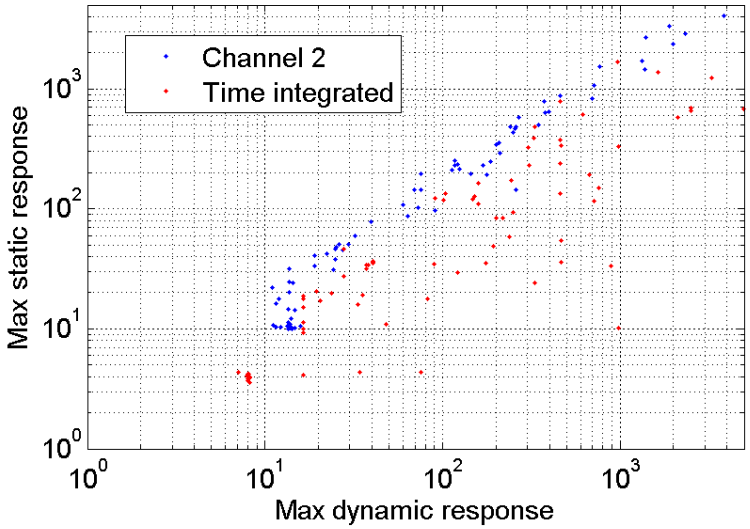

Figure 13: Comparison of the amplitude of the target response in dynamic and static acquisition modes.

Target response stage in static acquisition mode is displayed in Figure 14 as a function of target caliber with a 14 mV threshold. All unreliable inversion results are caused by weak target response and coincide with below-threshold RS value. For instance, the two deep 81 mm mortars discussed earlier and the 155 mm projectiles buried at 1.5 m (targets 32-33 in Figure 11) would remain undetected in dynamic search; their static response is too weak for data inversion. However, both 155mm buried at 1.19 m were successfully recovered although RS for one of them is below the threshold. At 15 mV, M42 targets buried at 0.35 m yielded poor inverted parameters whereas 0.80-m deep 105mm projectiles were successfully recovered. The time-integrated version of RS yields better inversion performance predictions (Figure 15). Unfortunately dynamic data was not collected on all deep calibration targets to confirm that definition (Figure 11 and Figure 16). In general, we can conclude that undetected targets during the dynamic search are not recoverable even with higher quality, cued interrogation static data.

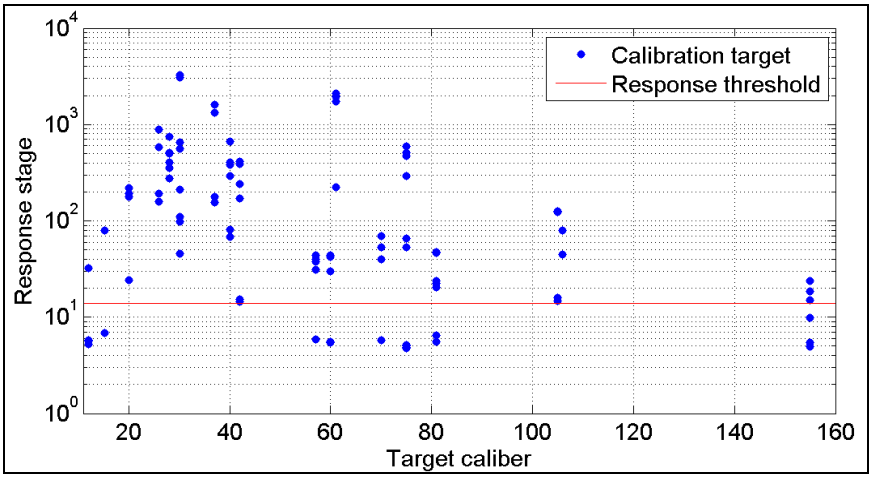

Figure 14: Response stage for calibration targets. The target response is computed as the norm of the recorded response among all receivers at the second time channel (same metric as submitted dig list). The detection threshold was set to 14 mV. Targets with caliber lesser than 20 correspond to test wire loops.

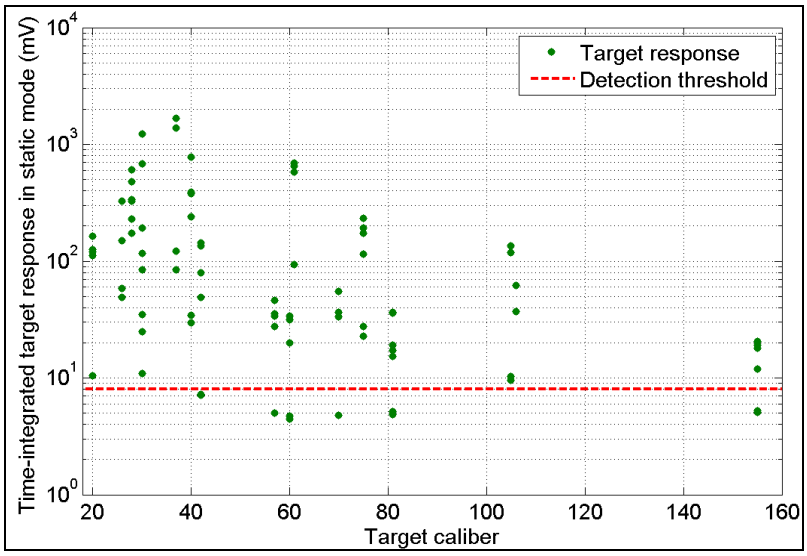

Figure 15: Time-integrated response as a function of caliber with an alternative threshold value. Deep M42 (42-equivalent caliber for convenience) are below threshold and yield poor inversion results, similar to the deepest 155m projectiles, whereas all 105mm projectiles are above threshold and successfully inverted.

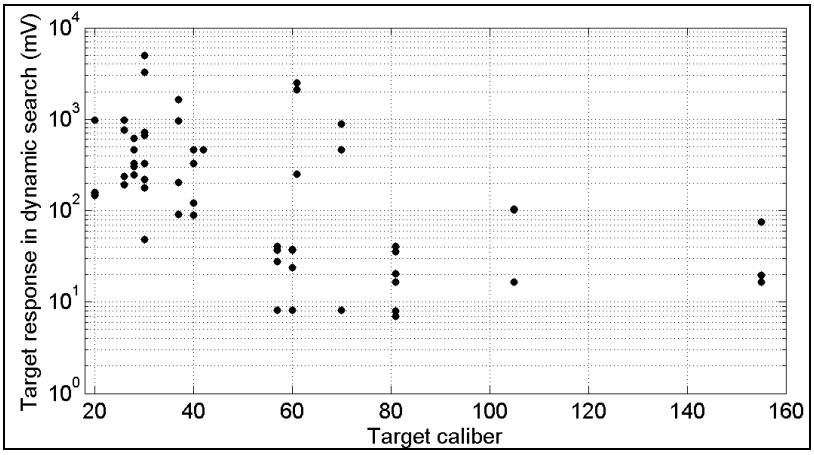

Figure 16: Time-integrated target response stage with dynamic data as a function of the target size. A dynamic detection threshold of 10 mV could be applied.

7.2 OBJECTIVE: MINIMIZE NUMBER OF FALSE DETECTIONS

Detection was achieved through the arrow display. This objective was attained by setting a null response of that display above regions where we knew that there was no metallic target. This task was facilitated with a priori knowledge that the site had been cleaned for surface clutter and only contained targets at cell centers. This background compensation operation can be saved; therefore this process can be applied to most sites as long as the field operator can identify a clear area; an in-air calibration is also valid if the soil response is negligible at the site.

7.3 OBJECTIVE: MINIMIZE NUMBER OF ANOMALIES TO REVISIT

An anomaly would need to be revisited is it was missed during the detection sweep and later identified through a detection quality control stage, or if inversion results suggest that

insufficient data were collected. Practically, only limited quality control was possible during the deployment because new aspects of the MPV integration with its positioning systems had not been immediately resolved to allow mapping and inversion. Detection control was first accomplished in the field by taking one static sounding at the center of each cell that had been qualified as empty and verify that the recorded response was similar to that of background. We found that we never had to reverse our diagnostic. Data collected through this process also provided material to compare dynamic and static responses (see previous section). This verification process is not applicable at a live site where target locations are unknown; therefore detection relies on operator's awareness and post-survey mapping. An automatic detection alarm could be implemented to second the field operator in identifying potential targets.

Anomalies would also need to be resurveyed if essential soundings were found to be corrupted or if analysis of data inversion results suggested that an incomplete set of cued interrogation soundings had been collected. The former was verified in the field by displaying each static sounding immediately after acquisition and controlled again at day end. Data sufficiency for inversion was not verified during deployment. However, that criterion was later assessed by verifying the stability of the recovered target location and polarizability parameters when varying the number of soundings used for inversion. Calibration data were inverted using one, two or three soundings. We found that the recovered parameters approached the final set of parameters obtained with all available soundings with just three soundings. Most of the calibration area and the entire blind grid were surveyed with an additional measurement in which the MPV was pitched backward. Data were inverted with and without that extra sounding. We found that the extra sounding had no effect on the calibration set whereas there were few instances of secondary polarizabilities alteration on the blind grid – in these cases we chose the most munitions-like solution.

7.4 OBJECTIVE: CORRECT CLASSIFICATION OF MUNITIONS

The main task in this objective is to separate munitions from clutter. The secondary task is to provide an adequate estimate of the target size. Probability of identifying buried UXO reaches 95% for shallow depth and 90% for medium depth (Table 5 of Appendix B). Probabilities are similar for detection and discrimination, indicating that most UXO were recognized as such. However, the probability of correctly identifying a UXO is 88% for small caliber and 57% for medium and large calibers (Table 7 of Appendix B). We first task is a success and the second task yields acceptable results when considering the relative difficulty of the classification challenge at YPG with the presence of 14 different UXO types and the adopted classification approach. The two tasks are intricately linked because, with so many UXO types, clutter rejection relies on the ability to correctly identify UXO types.

Previous ESTCP live site demonstration studies have involved at most 4 types of munitions to differentiate from a much larger set of clutter items. In these classification studies the UXO and non-UXO classes could be separated using two feature vectors, typically some size and time decay parameters. Each class would occupy a distinct region of model space with minimal overlap and a boundary could be defined. The problem becomes more complex with 14 UXO types that cannot be lumped into a single category because of the variety in target size and physical properties. Reducing classification feature vectors to two parameters offers too weak a separation (Figure 9, section 6.5). We chose to use the recovered sets of polarizabilities to allow our classifiers to incorporate additional model features, such as the relative decays of primary

and secondary polarizabilities, the similarity of secondary and tertiary polarizabilities for bodies of revolution. The relationship between these features was not imposed and left to non-linear classifier algorithms; however late-time secondary polarizabilities were omitted because they were often associated with weak signal and ill-constrained. Each munitions type only appeared in 3-6 usable instances on the calibration lanes, which provides too weak a sample size to fully assess in-class variability and prevent risk of over fitting the classifier. Therefore similar munitions were aggregated to form hybrid classes composed of 155-105mm, 81mm-2.75", 60-57mm, 37-40mm, 20mm-M75-BDU28 and M42-BLU26. Although statistically sounder, this method has one major drawback for scoring and gets penalized for mislabeling targets, for instance declaring a 60mm mortar instead of a 57mm. This explains our relative mediocre performance in that sector. This type of issues is less likely to occur at a live site, where the range of target types would be reduced. Besides, the small representation of target types and clutter imposed using a conservative approach to define the discrimination stage threshold to limit the risk of a false negative.

7.5 OBJECTIVE: REDUCTION OF FALSE ALARMS FOR DISCRIMINATION

This objective is closely related to the previous one. Mediocre performance can be attributed to the challenge of defining a classifier for 14 different types and the fact that clutter and munitions were represented in similar amounts in the Blind Grid, whereas there would be one-two orders of magnitude at a live site. The adopted classifier used 6 different types, which opens the possibility of mislabeling clutter if its recovered parameters lied between two UXO in-class end members. A conservative discrimination threshold was also adopted because of the problem complexity and the relative novelty of interpreting second-generation MPV data.

We found that the process of clutter rejection was further complicated by the potential occurrence of BLU-26, a pseudo-spheric submunition grenade with external rings. Most UXO had stable and well defined polarizabilities, especially at early time (Figure 10), with the notable exception of the BLU-26. Its recovered polarizabilities showed higher variability and crossovers because of its particular shape and generally weaker signal response. In contrast, #8 and #12 shots generally yielded stable, sphere-like polarizabilities. Small clutter could mistakenly be associated with BLU-26 and degrade classification performance. Separation of the secondary and tertiary polarizabilities for the 20mm projectile as early as 0.6 ms was also a potential source of misclassification (Figure 10).

7.6 OBJECTIVE: LOCATION ACCURACY OF BURIED MUNITIONS

Performance at prediction the target location and depth is presented in Figure 17. For the Calibration Lanes (left panel), the difference between the theoretical locations (cell center) and the predicted easting, northing and depth is well within the stated objective: the mean error is less than 0.01 m and standard deviation less than 0.07 m. For the Blind Grid the reported mean depth error is 0.01 m with a standard deviation of 0.09 m (Figure 17, left). The horizontal offsets with theoretical centers have 0.02 m mean and 0.10 m standard deviation.

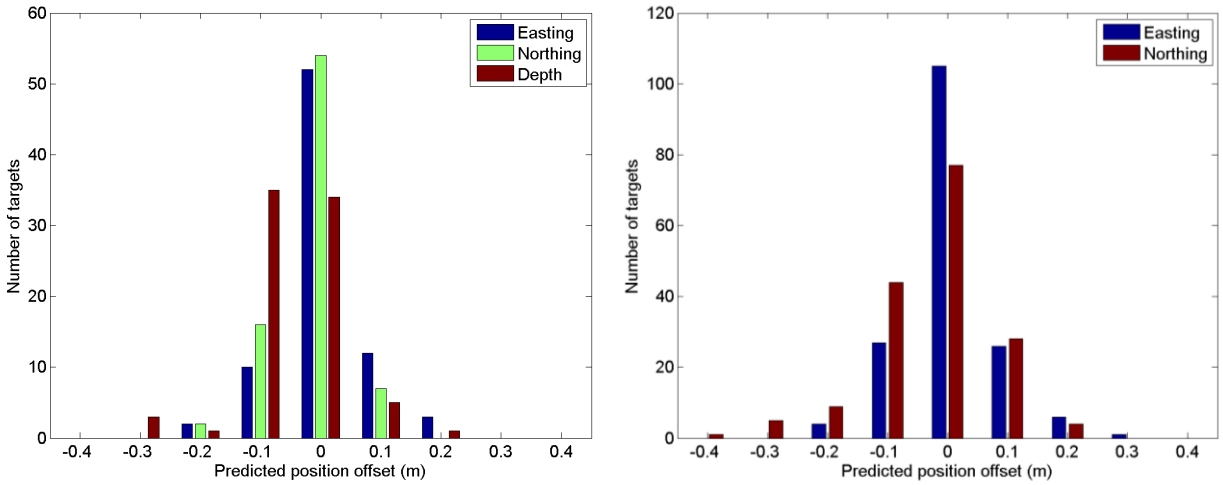

Figure 17: Predicted location accuracy. Left: Calibration Lanes; Right: Blind Grid.

7.7 OBJECTIVE: PRODUCTION RATE

The summary of daily activities is illustrated by Figure 18. It takes on average 3 minutes to characterize one anomaly, including setting up the beacon positioning system, and therefore we could expect to characterize 100 anomalies per day if the MPV were to be deployed for cued interrogation only. When including detection survey and regular operation downtime (battery change, system check, target management and personnel rest) we obtain an average of 6 minutes per target. Additional delays occurred during significant rainfall and when performing reconnaissance of the desert Extreme area.

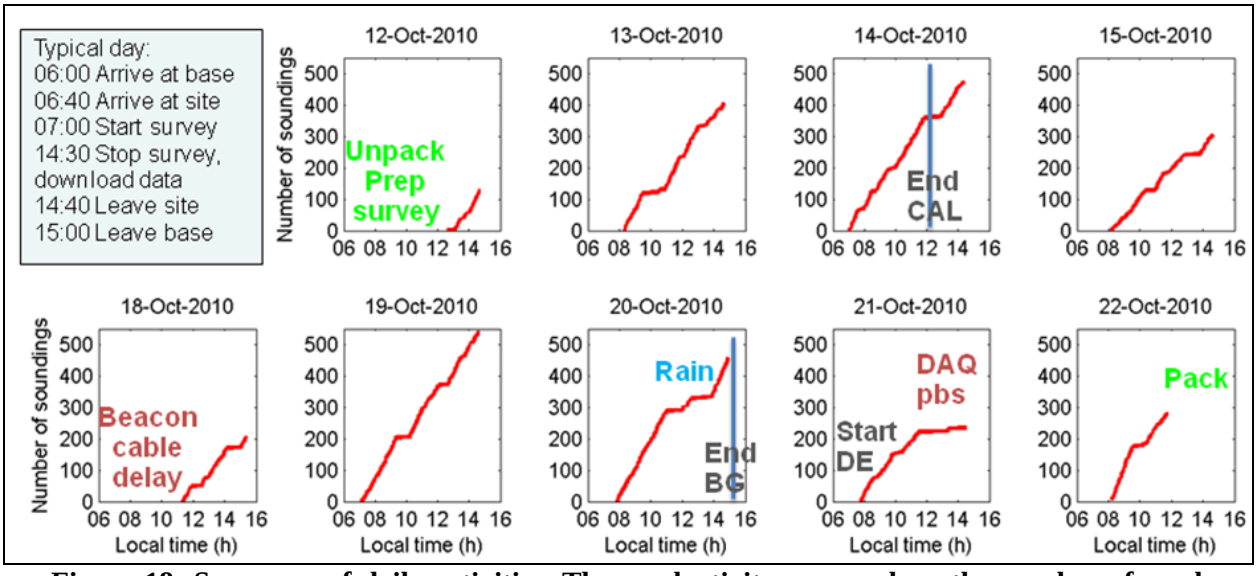

Figure 18: Summary of daily activities. The productivity curves show the number of cued interrogation soundings as a function of the data acquisition time. On average it takes 7-8 soundings to characterize one anomaly (one beacon boom location sounding and 5-8 soundings above the target). Productivity rate is reduced if there are few detected targets or if the survey is interrupted.

7.8 OBJECTIVE: EASE OF USE

A field geophysicist associated with Sky Research Operations was trained to survey with the MPV. The operator was instructed on starting and setting up the sensor, on running a detection survey, and finally on cued interrogation. The latter task is the most complex, as it involves analyzing the recorded signal for each receiver and component to build a mental image of the relative target and MPV head locations. This task is necessary to ensure that there is adequate spatial sampling of a target anomaly, for instance by verifying that one of the receiver units is sufficiently offset to measure the background response. Although the field operator performed satisfyingly, we are envisioning implementation of a signal mapping functionality at a later sensor development stage to facilitate and streamline this data collection process.

7.9 INVERSION OF DYNAMIC DATA

Data collection and site remediation could be accelerated if only a subset of the detected targets needed cued interrogation. When performing both the dynamic detection and static cued interrogation survey with the MPV productivity could be increased if the dynamic could be used to classify some of the potential targets. With that goal in mind and to further characterize the sensor we collected and inverted the dynamic data with a 2.6 ms acquisition window.

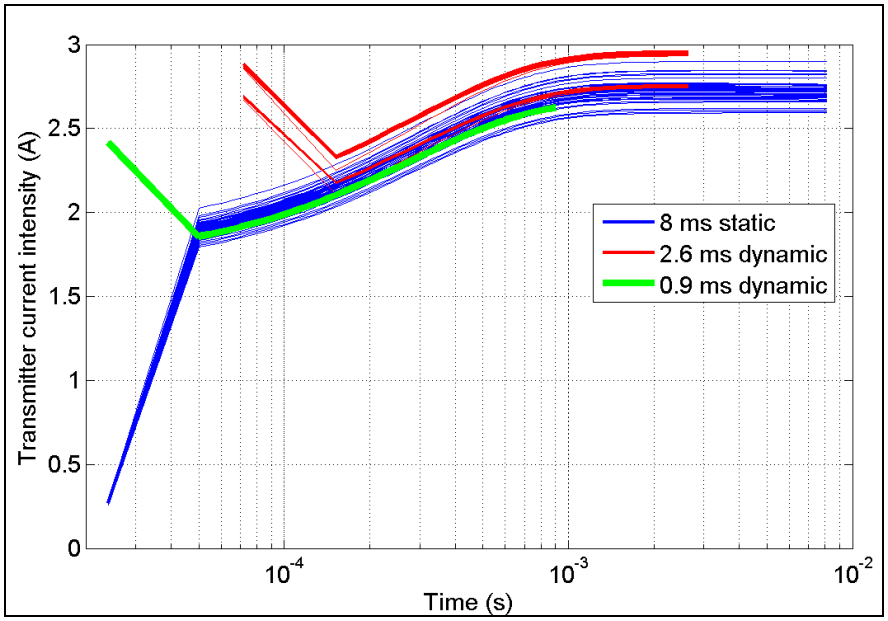

Figure 19: Transmitter current in dynamic and static acquisition mode. The transmitter quickly switches off to zero right after the latest time (the earliest recorded time and current value are measuring artifacts).

By default, the MPV and MetalMapper have been deployed with 0.9 ms excitation and transient recording during dynamic search. This setting implies 27 repeats of a 50% duty cycle alternating positive and negative stimulation (cycle duration of 3.6 ms) as part of 0.1 s data block – a short data block limits smearing the EMI response when moving the sensor. The data block duration can be preserved while achieving longer 2.6 ms excitation times with 9 repeats without significant noise degradation. The transmitter current waveform is shown in Figure 19 for 0.9, 2.6 and 8 ms excitation time. The MPV transmitter is still charging at 0.9 ms and approaching its maximum value (the MetalMapper is charged at 80% after 0.9 ms). The transmitter is fully

charged after 1.5 ms and keeps energizing the subsurface for an additional 1-6 ms for the 2.6 and 8 ms excitation times.

The difference between the saw-tooth and step-off waveforms greatly affects the target response. The 0.9 ms generates quickly vanishing signal whereas the 2.6-8 ms waveform fully energizes sub-surface targets and returns longer EMI transients. Inverted polarizabilities for data collected with both 2.6 ms (dynamic) and 8 ms (static) time decays over the same unknown targets are presented in Figure 20. Similar polarizability amplitudes and decay rates are obtained for the two modes. The difference in recorded depth (Figure 21), which directly affects polarizability amplitude, is less than 0.10 m for 85% of the tested targets. Most of the discrepancy is due to low SNR targets (notably targets A3, which is predicted deeper than 1 m for both datasets, and Q3 that has rapidly decaying signal – likely a piece of clutter). This is an excellent result given that inversion was not optimized to make best use of dynamic data (e.g., background response is negligible – see Appendix C – and was simply parameterized).

The fact that similar polarizabilities can be extracted in dynamic and static modes offers the possibility to utilize similar classification features and apply similar classification methods. Some level of dynamic-data-based target pre-screening could therefore be performed before cued interrogation data are collected.

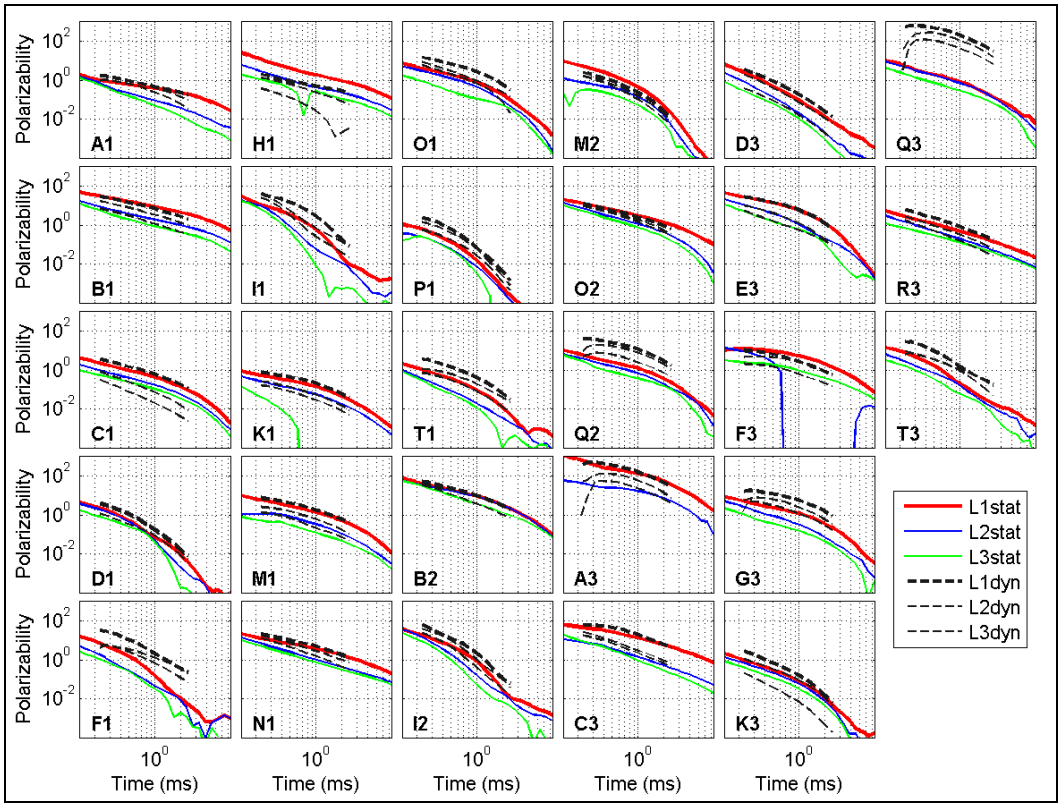

Figure 20: Recovered polarizabilities for anomalies surveyed in dynamic 2.6 ms dynamic acquisition and 8 ms static acquisition modes (only static was used for YPG demonstration scoring). Note that no background compensation was performed on dynamic data and therefore early time data were not inverted.

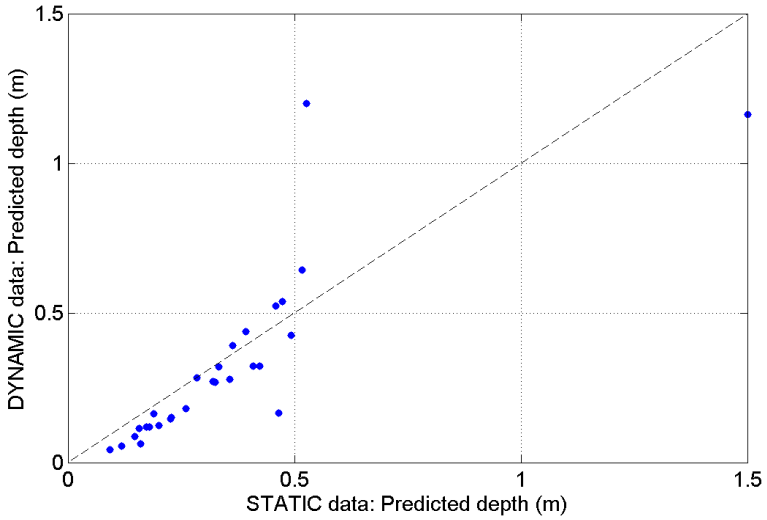

Figure 21: Predicted depth from inversion of static (cued interrogation) and dynamic (detection search) data.

7.10 ACCURACY OF BEACON POSITIONING SYSTEM

The survey at YPG was accomplished with both GPS and beacon positioning systems, thus allowing the MPV demonstration to proceed using the established GPS technology while testing the beacon for its accuracy, range and reliability. An attitude sensor was used to provide the MPV azimuth, pitch and roll. The beacon approach cannot resolve azimuth and therefore requires at least an auxiliary compass.

The Novatel RTK GPS has an accuracy of better than 1 cm for the horizontal location and approximately 1 cm for the elevation. The Honeywell attitude sensor is accurate to approximately 1 degree in all three angles. Given that the position and orientation sensors are attached to the MPV handle – approximately 1.3 m above and 1 m behind the MPV sensor head – and that there is 1-2 degrees mobility in the sensor head and handle assembly, the accuracy with locating the MPV position and orientation is degraded to 1-3 cm and 1-2 cm through the lever-arm effect. In contrast, the beacon method directly predicts the sensor head.

The method for inferring the MPV head location was presented in Lhomme et al. (2011). The magnetic field emitted by the MPV transmitter and measured at a beacon boom receiver is obtained by integrating Biot-Savart's Law. Using two sets of 3-component receivers one can recover the three positional parameters and the pitch and roll by solving a non-linear optimization problem. The solution relates the MPV location and orientation to that of the beacon boom. The orientation of the survey is obtained by measuring the beacon boom azimuth. The global position can be derived if the beacon boom is globally positioned.

At YPG we were able to compare the relative accuracy of the positions predicted with the GPS and beacon by comparing their corresponding survey patterns and minimizing the difference. An example of recovered locations at close range is shown in Figure 22. The furthest separation between a sounding and a receiver is 3.5 m and the overall accuracy remains within 2 cm in horizontal location and 2 cm in elevation.

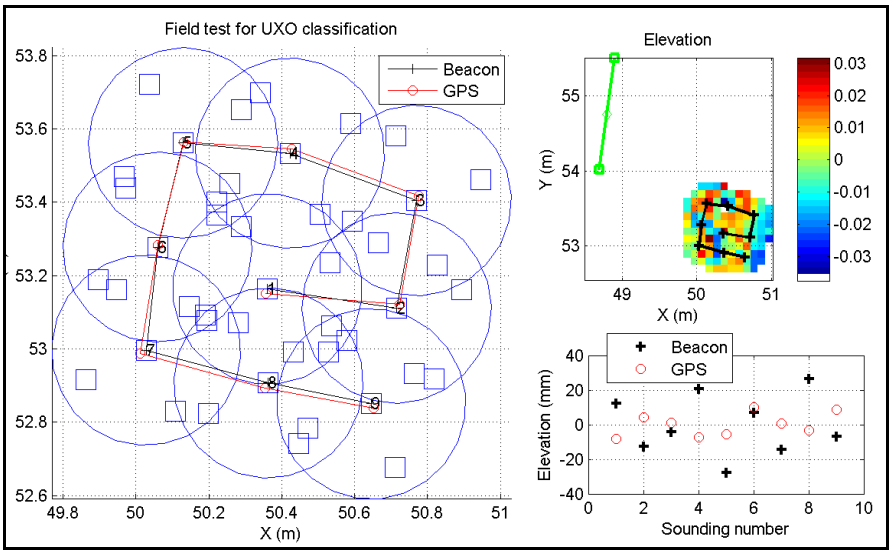

Figure 22: MPV sensor position with GPS and beacon for a 9-point cued interrogation. The left panel indicates the sensor head contour and cubes location for the beacon. The bottom right panel compares the relative predicted height for each sounding. The top right panel shows the position of the beacon boom (green line with cubes at either ends) relative to the cued interrogation pattern.

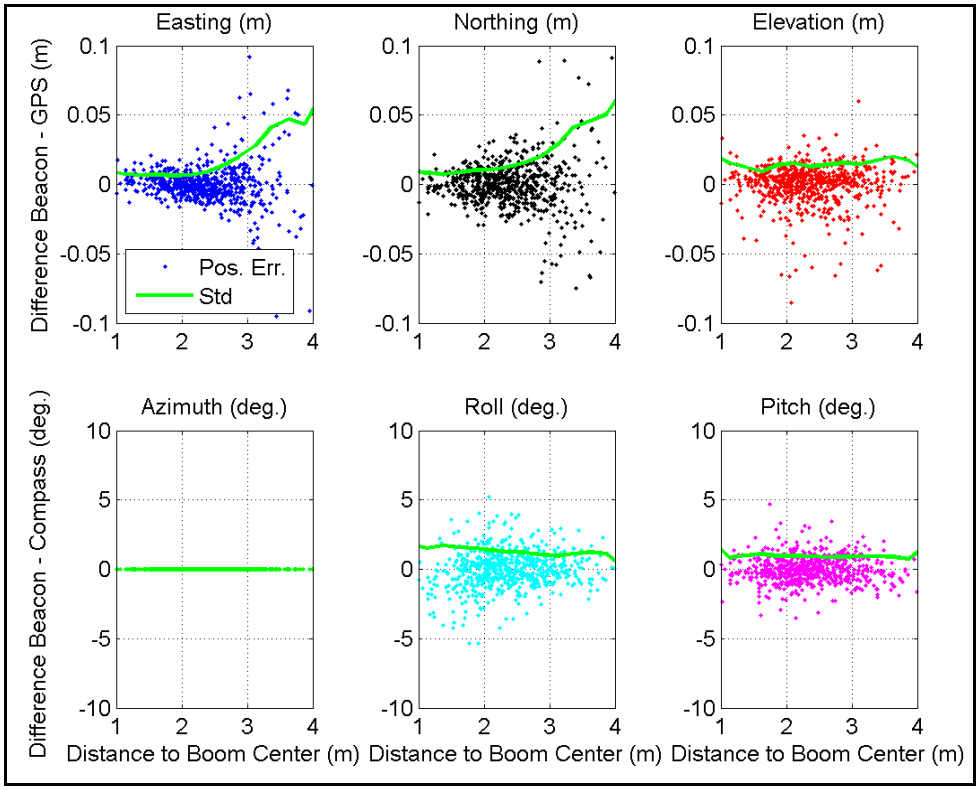

Figure 23: Relative accuracy of beacon positioning system. Results for 100 cued interrogations (700 stations) are obtained by minimizing for each cued interrogation the difference between the GPS and beacon position patterns. The top three pannels correspond to position; the lower three pannels compare with the attitude sensor. The azimuth was not recoverable from the beacon.

Comparison of the relative accuracy of GPS and beacon is presented in Figure 23. We find that the two positioning systems maintain their position and elevation within 2 cm and that the sensor measured and predicted attitude remain within 2 degrees in the 1-3 m range. To assess the required level of accuracy we re-inverted the GPS-positioned calibration data with added 2-cm and 2-degrees positional error (Figure 24). The recovered polarizabilities closely match the non-perturbed ones. This result suggests that this level of accuracy is satisfactory for geophysical inversion with the MPV sensor.

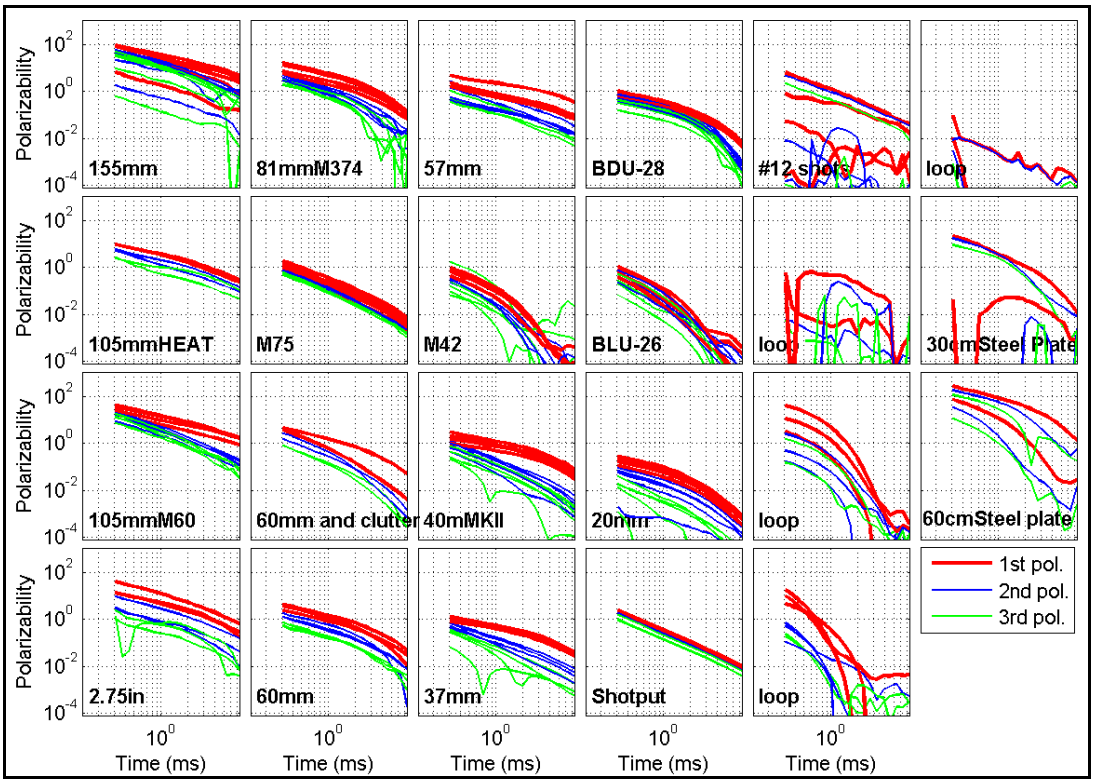

Figure 24: Recovered polarizabilities for targets at YPG calibration lanes after addition of 2-cm and 2-degrees positional error.

7.11 SENSOR RELIABILITY AND UPCOMING MODIFICATIONS

The sensor was fully operational most of the time. The detection indicators provided adequate information for an alert operator to detect a potential target, given that all targets which response exceeded the detection threshold were also detected in the field by the operator. In terms of hardware, we encountered two setbacks. First, the X-component of the center cube stopped functioning after 4 days. Its pre-amplifier circuit board, although protected inside the MPV head case, got damaged. We suspect that the MPV head incurred some flexing and thereby stained the nearby board. We expect that this issue will be avoided in subsequent deployments after replacing the transparent plastic top and bottom sheets with thicker, more rigid ones (1/8" Lexan instead of 1/16", with limited weigh increase) that close the MPV casing. The pre-amplifier boards will be placed further away from the casing. The second hardware incident occurred when cables for the beacon-boom receivers were pulled out of their DAQ connectors after getting caught in a survey peg, resulting in damage to both cable sets. The connectors

require precise assembly from a technically advanced electrical engineer; thus in-field repairs are not feasible. To prevent this problem in future demonstration cables will be secured and protected, and spares will be brought to the field.

Productivity losses also occurred at battery changes because of occasional computer port-mapping issues. Field control of the MPV computer is performed through a touch-screen display. For practical reasons we adopted an iPad, which can only communicate through wireless network. The DAQ also communicates with an attitude sensor and a GPS. We found that, at start up, the computer operating system would occasionally remap its ports, thus preventing the DAQ from communicating with one of the secondary sensors. G&G is currently investigating this problem, which is a new issue that occurred upon upgrading to a Windows 7 operating system.

8.0 COST ASSESSMENT

The costs presented reflect the costs incurred to date to complete system modifications, software modifications and upgrades, shakedown testing, and deployment and analysis of data collected at the YPG Standardized UXO Test Site. The costs for the YPG deployment are considered to be higher than would be representative of costs for deployment in a full production mode as there were some instrument issues that had to be addressed in the field that prolonged the data collection. Additional time was spent on data analysis to extend the MPV characterization study. For instance we analyzed dynamic data to assess the potential to carry detection mapping and invert the collected for target classification. We also studied the performance of the beacon positioning system.

8.1 COST MODEL

The cost breakdown for the cost elements tracked since project inception is presented in Table 4. Costs are presented by total labor hours, subcontract, materials, and travel. Some modifications were performed under SERDP 1443, the project led by CRREL to develop the MPV, as well as funds that were added to SERDP 1637 for development and testing of the positioning beacon. Because the costs to date include development costs and the YPG survey wasn't necessarily representative of a typical deployment, we have not calculated per anomaly costs.

Table 4: Cost breakdown for MPV demonstration study.

Cost Element	Data Tracked During Demonstration	Estimated Costs
Instrument Cost	*Modifications to the MPV sensor head and electronics:*	
	Labor	185 hours
	Subcontract	$22,244
	Materials costs	$12,383
	Shakedown testing at G&G location:	
	Labor	96 hours
	Subcontract	$13,800
	Materials/Supplies	$100
	Travel	$945
Demonstration Plan preparation	*YPG UXO Test Site Application and ESTCP Demonstration Plan*	
	Labor	120 hours
Demonstration Preparation, Mobilization & Demobilization	*YPG Deployment: Preparation of software and logistics*	
	Labor	120 hours
	Travel	$2450
	Shipping & supplies	$100
Site Preparation	*Not Applicable* – standardized UXO test site at YPG	

Cost Element	Data Tracked During Demonstration	Estimated Costs
Survey Costs	*YPG Site Survey* Labor Travel 7 per diem costs (2 SKY employees) Subcontract Materials/field supplies	 201 hours $4,300 $23,594 $172
Detection and Discrimination Data Processing	*Data processing and analysis* Labor	 340 hours
Report Preparation	*YPG Demonstration Report* Labor	 80 hours
Estimated total costs		**$272,000**

Instrument costs: several modifications and enhancements to ruggedize the MPV and reduce weight and make it easier to deploy were completed. Some system components were also upgraded, including a new chassis, DAQ, controller, and ancillary components. The modifications were performed by G&G Sciences, and included coordination with the SKY PI and CRREL developer. Activities performed in coordination with the system enhancements included analyzing the data quality and fully characterizing the noise characteristics with the goal to ensure that the modifications would optimize performance.

Demonstration plan preparation: Documents required to prepare for the YPG deployment included preparation of the YPG Standardized UXO test site application, and an abbreviated ESTCP Demonstration Plan.

Demonstration Preparation, Mobilization & Demobilization: Preparation activities for the YPG site deployment included preparation of all pre- and post-processing software for the MPV and beacon analysis, coordination with the YPG test coordinator, packing and shipping the MPV, and travel to and from Yuma.

Survey costs: The survey was conducted over 9 days. Two SKY staff were on-site for the duration, as well as the CRREL scientist and G&G Sciences electrical engineer. Cost items include labor, per diem, and field supplies.

Detection and Discrimination Data Processing: Data processing and analysis activities included initial pre-processing, analysis of the positioning beacon data, and processing the sensor data for both cued and dynamic data. A dig sheet was submitted to the YPG coordinator for scoring as soon as possible following completion of the field survey. Analysis of the data included inversion and classification using various techniques, and the data were also analyzed using non-dipole methods developed under SERDP 1572. The analysis therefore included coordination with the SERDP 1572 PI and comparison of the non-dipole classification results and dig list with those obtained using the dipole methods.

As noted, the costs to complete the YPG demonstration are not considered fully representative as some instrument issues that were resolved in the field prolonged the survey, and the processing and analysis costs reflect additional effort needed to evaluate multiple options for classification and error analysis. We anticipate that the efforts to fully characterize the data and error analysis performed for the YPG data will help optimize the approach to be used for the upcoming Camp

Beale demonstration. Costs for that effort should be much more representative of the costs required to deploy the MPV in a production setting.

8.2 COST DRIVERS

The MPV was developed to provide a moderate cost, reliable, portable sensor with advanced discrimination capabilities that can operate at sites with challenging surveying conditions. As a portable system, deployment logistics and costs for transport and operation are quite low relative to towed arrays or other vehicular-based systems. The primary costs are incurred for labor and travel for the operators, and the primary cost driver becomes the duration of deployment, directly related to the acreage to be surveyed as well as the difficulty of the terrain (steep, rocky, very uneven, and wooded terrain will take somewhat longer to survey than just because its more difficult to hike across these areas).

8.3 COST BENEFIT

The primary driver for developing the MPV is to make discrimination feasible at a wide range of sites where field conditions prohibit the use of cart-based systems, and for small-scale deployment where a small area needs to be surveyed or where anomalies need to be resurveyed at a lower cost than a cart-based system.

9.0 IMPLEMENTATION ISSUES

The MPV2 is a research prototype. The sensor is operable in the context of live site demonstration with the assistance of advanced geophysicists. Because the sensor is an early prototype there is no user manual available yet. We plan to produce such type of document, including basic fool-proofing and trouble-shooting, as part of the next demonstration. Sensor reliability issues, discussed in an earlier section, are being addressed whenever these arise. Other potential issues are discussed below:

- We are not aware of any environmental regulations and any necessary permits related to surveying with the MPV technology. Access to GPS radio frequency is convenient but not necessary.
- Previous concerns were related to the weight, size and fragility of the sensor. The new sensor head design is significantly lighter and sturdier. The sensor can be operated by the same person for an entire day.
- The sensor is still at a prototype stage. The instrument can currently only be custom made by G&G Sciences. The DAQ is made of National Instrument components that are available by order (with delays).
- There is only one instance of the MPV2 sensor. Additional sensor could be made available, depending on G&G Sciences.
- Operation of the MPV technology requires training from one of the scientists that participated in this demonstration. Data processing requires advanced UXO data interpretation experience.

10.0 REFERENCES

Barrowes, B.E., Recent advances in Vector EMI Sensors, ESTCP SERDP/ESTCP Partners in Environmental Technology Symposium, Wash., DC, Dec. 2007a.

Barrowes, B.E., O'Neill K, George, D.C., Snyder, S., Shubitidze, F. and Fernandez, J. P., Man-Portable Vector Time Domain EMI Sensor and Discrimination Processing, SERDP 1443 FY07 Annual Report, 2007b.

Bell, T. H., Barrow, B. J. and Miller, J**.** T., Subsurface discrimination using an electromagnetic induction sensor, IEEE Transactions on Geoscience and Remote Sensing, 39, 1286–1293, 2001.

Bell, T., Geo-location Requirements for UXO Discrimination, SERDP Geo-location Workshop, 2005.

Billings, S., Pasion, L**.,** Lhomme, N. and Oldenburg, D., Discrimination at Camp Sibert using Time-Domain EM, SERDP/ESTCP Partners in Environmental Technology Symposium, Wash., DC, Dec. 2007.

Fernandez, J. P., Barrowes, B. E., Bijamov, A., Grzegorczyk, T., Lhomme, N., O'Neill, K., Shamatava, I., and Shubitidze, F., MPV-II: an enhanced vector man-portable EMI sensor for UXO identification, Proc. SPIE 8017, 2011.

Gasperikova, E., Smith, J. T., Morrison, H. F. and Becker, A., BUD results from the ESTCP Demonstration sites. SERDP/ESTCP Partners in Environmental Technology Symposium, Wash., DC, Dec. 2007

Gasperikova, E., Smith, J. T., Morrison, H. F., Becker, A., and Kappler, K., UXO detection and identification based on intrinsic target polarizabilities: Geophysics, 74, B1-B8, 2009.

Grzegorczyk, T. M., Barrowes, B. E., Shubitidze, F., Fernández, J. P., Shamatava, I. and ONeill, K. A.: Detection of multiple subsurface metallic targets using the man-portable vector EMI instrument. Proceedings of SPIE Defense+Security, Orlando, FL, April 2009.

Kingdon, K. A., Pasion, L. R. and Oldenburg, D. W., Investigating the Effects of Soils with Complex Magnetic Susceptibility on EMI Measurements Using Numerical Modelling of Maxwell's Equations, Proceedings of SPIE Defense+Security, Orlando, FL, April 2009.

Lhomme, N., Pasion, L., Billings, S. and Oldenburg, D., Inversion of frequency domain data collected in a magnetic setting for the detection of UXO, Proceedings of SPIE Defense+Security, Orlando, FL, March 2008.

Lhomme, N., Barrowes, B. E. and George, D. C., EMI sensor positioning using a beacon approach. Proceedings of SPIE Defense, Security+Sensing, Orlando, Florida, April 2011.

Pasion, L. & Oldenburg, D., A Discrimination Algorithm for UXO Using Time Domain Electromagnetics: Journal of Engineering and Environmental Geophysics, 28, 91-102, 2001.

Pasion, L., Billings, S. and Oldenburg, D., Improving Detection and Discrimination of Buried Metallic Objects in Magnetic Geologic Settings by Modeling the Background Soil Response. Proceedings of SPIE Defense+Security, Orlando, FL, March 2008.

Pasion, L., Kingdon, K. amd Jacobson,J., Simultaneaous Inversion of Electromagnetic Induction Data for Target and soil Parameters, Presentation at SPIE Defense, Security+Sensing, Orlando, Florida, April 2011.

Shubitidze, F., Barrowes, B. E., Shamatave, I. and O'Neill, K., Application of the NSMC model to the multi-axis time domain EMI data. SPIE Defense+Security, Orlando, FL, March 2008.

Smith, T.J. and Morrison, H.F., Optimizing receiver configurations for resolution of equivalent dipole polarizabilities in situ. IEEE Trans. on Geosci. and Rem. Sens., 43(7), 2005.

YPG Layout Description, http://aec.army.mil/usaec/technology/uxo01c02.html

APPENDICES

Appendix A: Points of Contact

Points of contact (POC) involved in the demonstration are listed in the following table.

POINT OF CONTACT Name	ORGANIZATION Name Address	Phone Fax E-mail	Role in Project
Dr. Nicolas Lhomme	Sky Research Inc. 112 A, 2386 East Mall, Vancouver, BC V6T 1Z3, Canada	Tel: 541-552-5180 Fax: 604-221-1055 Nicolas.lhomme@skyresearch.com	PI
Dr. Benjamin Barrowes	72 Lyme Road, Hanover, NH 03755-1290	Tel:(603)646-4822 Fax:(978)702-0448 benjamin.e.barrowes@usace.army.mil	Co-investigator
David George	G&G Sciences, Inc. 873 23 Rd Grand Junction, CO 81505	Tel: (970) 263-9714 Fax: (970) 263-9714 dgeorge@ggsciences.com	Co-investigator
Dr. Herb Nelson	ESTCP Program Office ESTCP Office 901 North Stuart Street, Suite 303 Arlington, VA 22203-1821	Tel: 703-696-8726 Herbert.Nelson@osd.mil	ESTCP Munitions Management Program Manager

Appendix B: Scoring report for YPG demonstration

Preliminary Data/No QA or QC

4.3 PERFORMANCE SUMMARIES

Results for the open field test broken out by size, depth, and nonstandard ordnance are presented in Table 5 (for cost results, see section 5). Results by size and depth include both standard and nonstandard ordnance. The results by size show how well the demonstrator did at detecting/discriminating ordnance of a certain caliber range (see app A for size definitions). The results are relative to the number of ordnance items emplaced. Depth is measured from the geometric center of anomalies.

The RESPONSE STAGE results are derived from the list of anomalies above the demonstrator-provided noise level. The results for the DISCRIMINATION STAGE are derived from the demonstrator's recommended threshold for optimizing UXO field cleanup by minimizing false digs and maximizing ordnance recovery. The lower 90-percent confidence limit on probability of detection and probability of false positive was calculated assuming that the number of detections and false positives are binomially distributed random variables. All results in Table 5 have been rounded to protect the ground truth. However, lower confidence limits were calculated using actual results.

TABLE 5. SUMMARY OF BLIND GRID RESULTS FOR THE MPV/HANDHELD

Metric	Overall	Standard	Nonstandard	By Size			By Depth, m		
				Small	Medium	Large	< 0.3	0.3 to <1	>= 1
RESPONSE STAGE									
P_d	0.85	0.90	0.80	0.95	0.75	0.80	1.00	0.90	0.00
P_d Low 90% Conf	0.79	0.79	0.68	0.89	0.59	0.58	0.94	0.76	0.00
P_d Upper 90% Conf	0.91	0.94	0.91	1.00	0.86	0.92	1.00	0.96	0.28
P_{fp}	0.95	-	-	-	-	-	0.95	0.95	N/A
P_{fp} Low 90% Conf	0.92	-	-	-	-	-	0.92	0.83	N/A
P_{fp} Upper 90% Conf	0.98	-	-	-	-	-	0.99	0.98	N/A
P_{hn}	0.00	-	-	-	-	-	-	-	-
DISCRIMINATION STAGE									
P_d	0.85	0.85	0.80	0.95	0.75	0.80	0.95	0.90	0.00
P_d Low 90% Conf	0.77	0.77	0.68	0.85	0.59	0.58	0.90	0.76	0.00
P_d Upper 90% Conf	0.90	0.93	0.91	0.98	0.86	0.92	1.00	0.96	0.28
P_{fp}	0.65	-	-	-	-	-	0.60	0.75	N/A
P_{fp} Low 90% Conf	0.58	-	-	-	-	-	0.53	0.64	N/A
P_{fp} Upper 90% Conf	0.70	-	-	-	-	-	0.68	0.87	N/A
P_{hn}	0.00	-	-	-	-	-	-	-	-

Response Stage Noise Level: 14.
Recommended Discrimination Stage Threshold: 24.

Note: The recommended discrimination stage threshold values are provided by the demonstrator.

Preliminary Data/No QA or QC

Appendix C: Background response with dynamic data

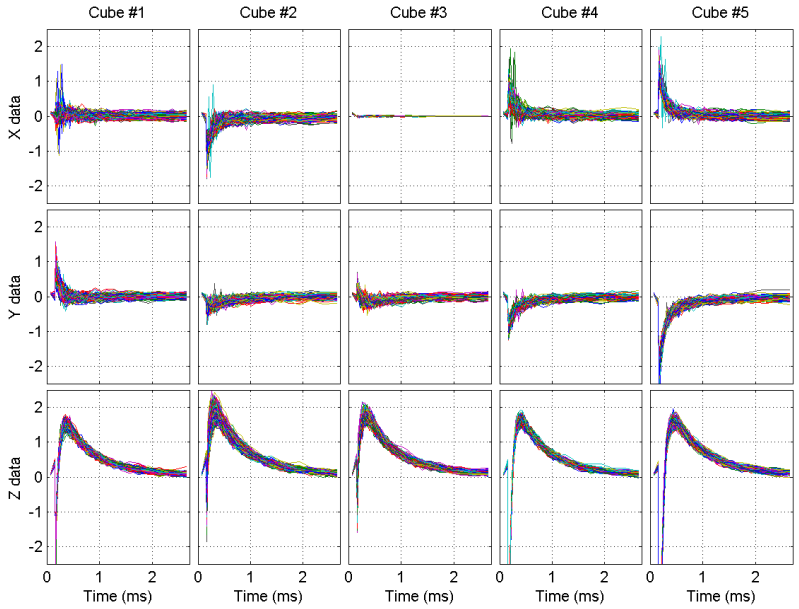

Figure 25: Background response over an empty cell in dynamic search.

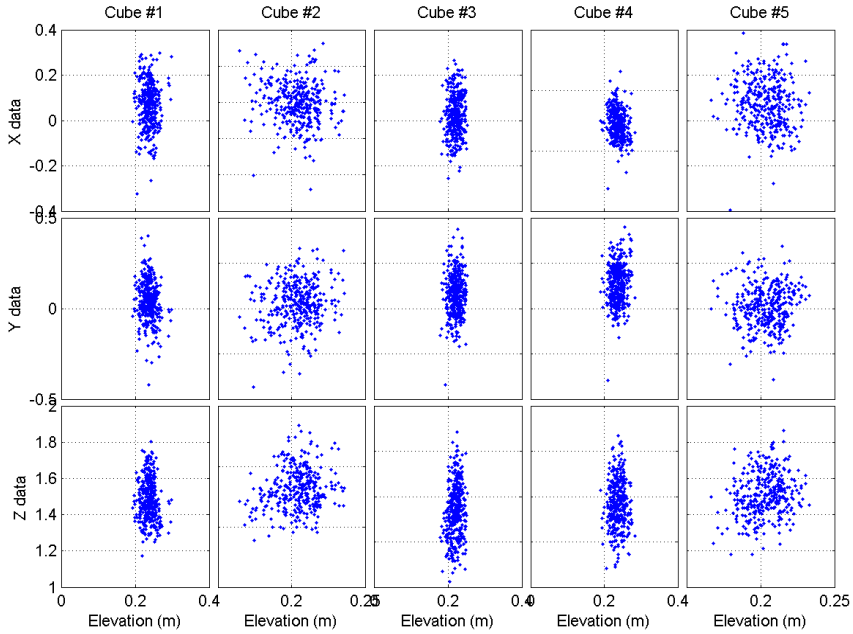

Figure 26: Background response (0.35 ms time channel) as a function of relative elevation (somewhat equivalent to height above ground because surface is mostly flat).

The EMI response over empty cells was studied to measure the amplitude and effect of the background response. Figure 25 shows that background has weak response with dynamic data. Figure 26 shows that there is no correlation between background response and ground clearance; therefore soil has a negligible effect on background response and most of the noise is intrinsic to the sensor. In conclusion, there is no need for any height correction when removing the background response.

Appendix D: MPV redesign analysis

The original MPV research prototype was modified in the spring of 2010 in preparation for field testing and demonstration at live sites to be conducted as part of ESTCP projects MR-201005 and MR-201158. The MPV design was revised to obtain a lighter, more maneuverable and sturdier sensor head.

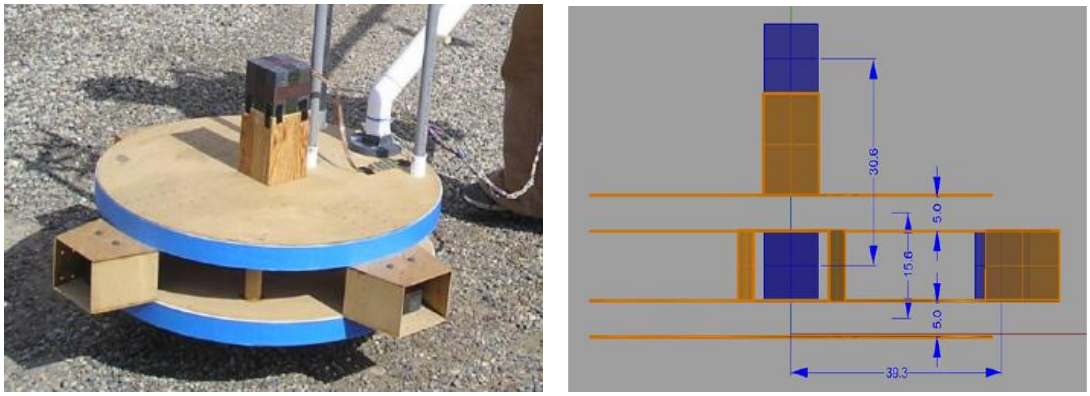

Figure 27: Original MPV sensor head design (head weight: 23 lbs).

The original design was built out of wood and Styrofoam (Figure 27). It consisted of a top and a bottom disk around which the transmitter coils were wound. Receiver units consisted of cubes with three sets of orthogonal induction coils (vector receivers). Four cubes were placed between the disks: one at the center and one on each of the right, left and front sides. The lateral cubes were placed inside a protruding wood enclosure such that the cube could be moved in and out of the transmitter disk for experimentation. The enclosures considerably increased the bulk of the overall sensor package. The wood material was extremely fragile, snag-prone and susceptible to damage. An additional cube was mounted 30 cm above the center cube.

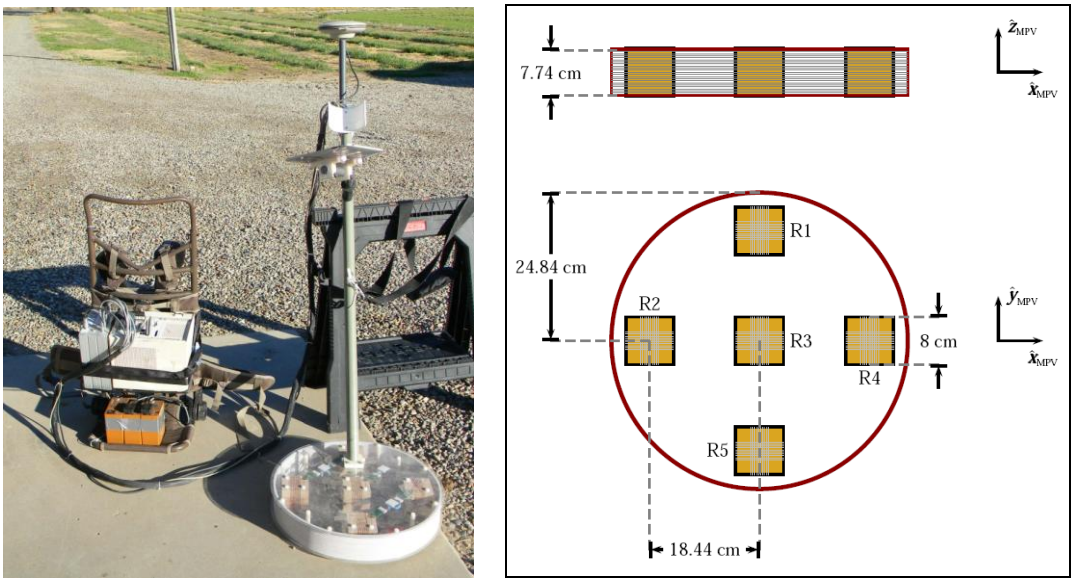

Figure 28: Second generation MPV design (head weight: 12 lbs).

D.1 Sensor head modifications

Several elements were modified:

- The sensor was simplified and streamlined to a single circular enclosure that contains all components;
- External enclosures were eliminated to obtain a smoother sensor profile that would not break or catch obstacles;
- Lateral cubes were brought inside the enclosure. Cube separation was reduced from 39 cm to 18 cm (between cube centers). *A priori* there is no particular advantage or caveat in reducing cube separation on the sensor as long as the survey protocol ensures that adequate spatial sampling of the anomaly is obtained during target interrogation. Reduced separation could be an advantage if gradient measurements were to be used, for instance for soil modeling because soil properties would more likely be homogenous;
- The top cube was relocated. The cube had limited purpose because it received weaker signal (see analysis hereafter). The cube was moved inside the transmitter disk and placed at the back of the enclosure on the same plane as the other cubes to obtain a symmetric cross pattern of receiver cubes;
- The top and bottom transmitters were merged into a single transmitter loop wound around the disk that hosts all cubes. In that manner both transmitters are closer to the ground and therefore send more energy to the buried target; this also brings the receiver cubes 5 cm closer to the ground as they no longer sit on top of the lower receiver disk;
- The transmitter diameter was reduced from 75 cm to 50 cm to improve maneuverability and accessibility and reduce weight. Analysis of the relative performance is detailed hereafter;
- Receiver cube size was reduced from 10 cm to 8 cm. The data quality is similar – the receiver coils essentially behave like point receivers. Balsa wood was used instead of solid plastic;
- Wood and Styrofoam were replaced with two sheets of transparent Lexan plastic on top and bottom.

The new design offers several handling benefits:

- Weight reduction: The new sensor head is 12 lbs, as opposed to 23 lbs previously;
- Improved maneuverability: Reduced swing weight with a more compact design;
- One-arm handling: Sensor head and control display are light enough to be operated with a single arm;
- Lower profile and smooth contour, less prone to catching branches and plants
- Increased solidity;
- Lower sensitivity to humidity owing to use of plastic casing instead of wood;
- Safer and more efficient operation with transparent casing that greatly reduces blind spots; ground surface obstacles and markers can be seen through the casing;
- Visibility of inside components for verification;
- Easier access to components for modification or repair.

Figure 29: MPV2 field data collection. Surveying generally requires two persons. The main operator carries the sensor with one arm and interacts with the control interface display with his spare hand. The second operator carries the DAQ backpack, takes field notes and monitors the survey for any potential difficulty.

The following sections provide a quantitative analysis of the expected new sensor performance.

D.2 Effect of top cube

In the original MPV, a cube was placed above the center cube to offer the possibility of taking gradient measurements. The top cube was supposed to be less sensitive to the effect of magnetic soil and to small clutter because these signals would be negligible at an elevated standpoint. Data collected with the original MPV were inverted with and without utilizing the top receiver cube. We find that the recovered target parameters are very similar (Figure 30) and that utilization of the top cube does not improve the stability of the recovered parameters. This is mostly due to the much weaker signal strength at the top cube because EMI fields decay proportionally to the inverse distance cubed. For example, the signal at the top cube is 8 times weaker than the signal at the center cube for a target placed 0.15 m below the sensor when accounting for the fact that the center cube already is 0.13 m above the sensor base. The expected benefits for magnetic soil can be addressed through modeling, especially when accounting for the fact that the center cube and the tangential components of the lateral cubes are completely immune to a locally uniform magnetic soil (Pasion et al., 2011 and Figure 5 in main body of this report). We decided that the benefits of the top cube were negligible and that this cube would serve a better purpose if placed on the same plane as the other ones where the signal strength is higher. We placed the cube at the back of the sensor to obtain a symmetric receiver pattern.

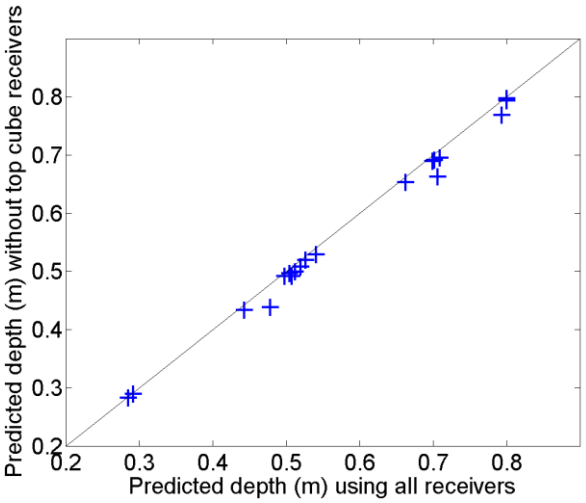

Figure 30: Effect of top receiver cube on recovered target parameters.

D.3 Reduction of transmitter diameter

Reducing the transmitter radius diminishes the amplitude of the illuminating magnetic field at depths exceeding the transmitter radius, which in turn reduces the maximum investigation depth. At shallow depth the magnetic flux is stronger as field lines are compressed into a smaller loop. These geometric effects need to be put in context with other redesign aspects. In particular, the proposed MPV2 design has transmitters and receivers as close as possible to the ground whereas the original MPV has the top transmitter 0.2 m above the sensor base and the receiver cube centers are 0.14 m above the base (0.045 m for the MPV2).

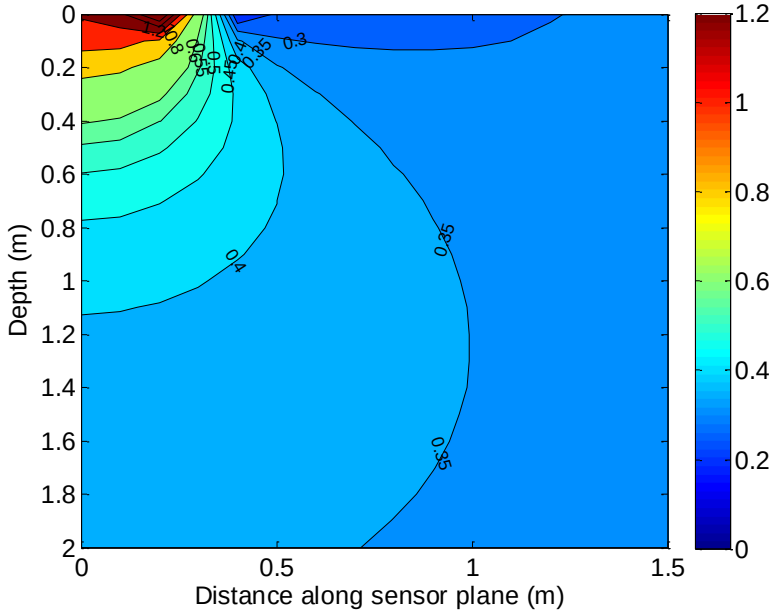

Figure 31: Ratio of primary field intensity between MPV2 and MPV sensor designs. The bottom of the MPV/MPV2 is considered as reference depth 0. The sensors have respectively 0.50-m and 0.75 m-diameter transmitter loop. Primary field is obtained by numerical integration of the Biot-Savart law and shown as a function of depth and horizontal distance from center of sensor base.

The ratio of the MPV2 and MPV primary field intensity as a function of depth below each sensor is shown in Figure 31. The primary field intensity for each sensor is shown in Figure 32 and Figure 33. The primary field is expectedly weaker for the MPV2, for instance by a factor 2.2 at 0.8 m depth. However, the difference is relatively negligible when considering that the target response is in turn attenuated as the inverse distance cubed – signal for a target at 0.8 m depth would be reduced by 25% or 2.3 dB.

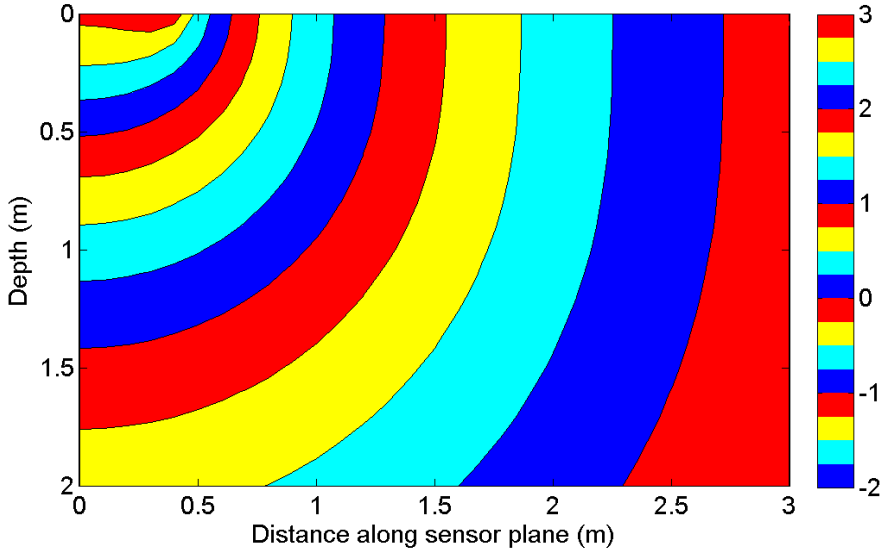

Figure 32: Intensity of primary field for the original MPV constituted of two 75 cm circular loop transmitters (here we show the decimal logarithm of the norm of the primary field). Zero depth corresponds to sensor base.

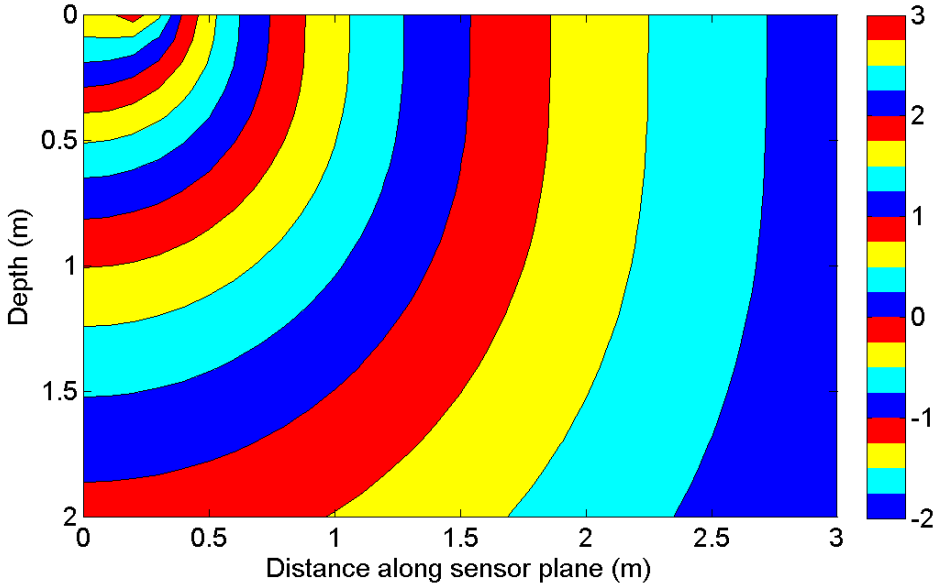

Figure 33: Primary field for proposed MPV2 design using 50 cm circular loop (here we show the decimal logarithm of the norm of the primary field). Zero depth corresponds to sensor base.

D.4 Expected classification performance for the new system

Simulations were performed to verify that the proposed new MPV design would satisfy the data quality requirements for UXO classification with a man-portable system. Namely, we expect the ability to characterize buried ammunitions within 1-meter depth when the burial depth is less than eleven times the caliber size. We also verified that performance would not significantly degrade, if at all, relative to the original sensor by reducing the geometrical dimensions of the new sensor.

We tested the potential at recovering 81 mm mortars and 37 mm projectiles near the theoretical maximum detectable depth. We considered a 3×3 grid point survey with 0.6 m horizontal spacing, which corresponds to 0.2 m-separation between receivers along the main directions given the receiver layout on the sensor (Figure 34). We also tested a reduced 5-point pattern with 0.35 m station spacing. The sensor was placed 0.05 m above the ground. Additional position and orientation errors were normally distributed with standard deviation of 1 cm and 1 degree and increased to 2 cm and 2 degrees to assess the effect of positional error on parameter stability. Additional EM noise was obtained by convolving the typical sensor background noise and a standardized normal distribution.

Target parameters were inferred from our library of polarizabilities for typical ATC 37 mm projectiles and 81 mm mortars. The target could lie at any orientation – azimuth, pitch and roll – and location within a 10 cm radius of the survey center with equal probability. Burial depth varied around 11 times the target diameter. Each test sample of simulated data was based on a new random realization of the target and survey parameters.

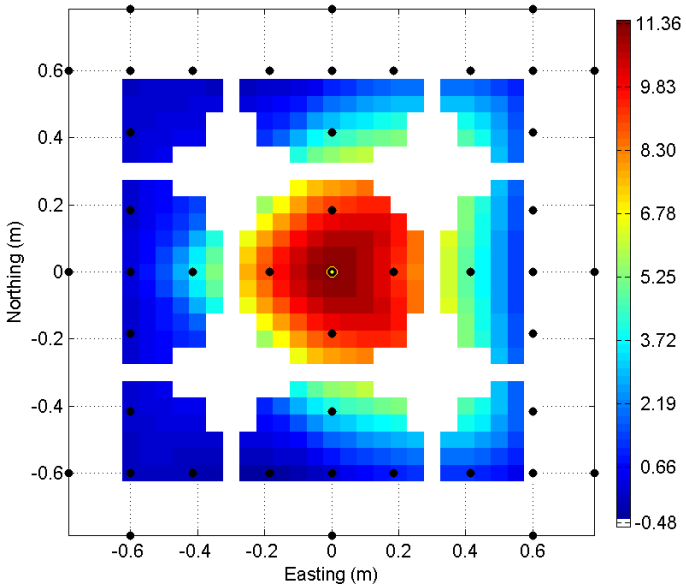

Figure 34: Survey pattern for simulations with new MPV design.

Synthetic data were inverted to recover the target location and polarizability parameters. Results for the 9-point pattern are presented and discussed in Figure 35, Figure 36 and Figure 37; in the latter figure, survey errors were doubled. Results in Figure 35 and Figure 36 show that the MPV2 is expected to allow reliable classification of 37 mm and 81 mm caliber ammunitions under the

commonly accepted 1-cm and 1-degree accuracy requirements when the targets are buried as deep as 12 times their diameter.

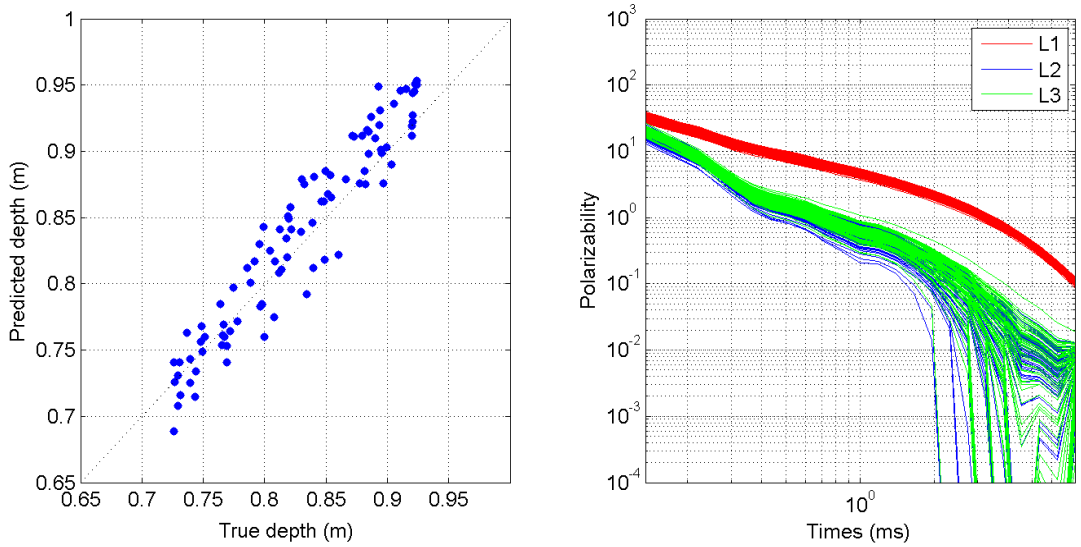

Figure 35: Simulated performance of MPV2 for the recovery of 81 mm mortars. Depth is recovered within 0.05 m. The main polarizability (L1) and secondary polarizability (L2, L3) decay curves are consistent and exhibit limited variability, which suggests the potential for reliable and efficient classification.

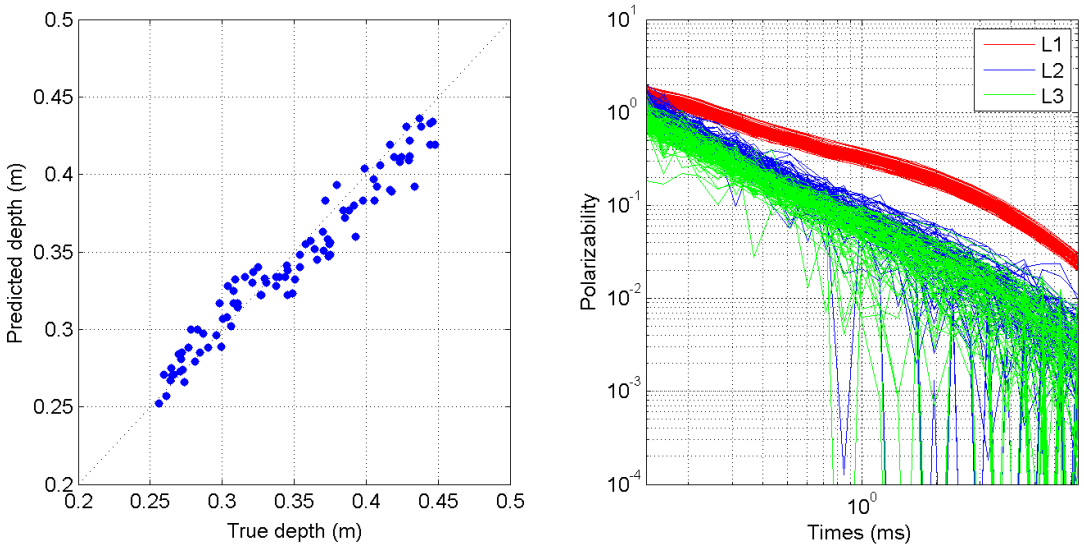

Figure 36: Simulated performance of MPV2 for the recovery of 37 mm projectiles. Depth is recovered within 0.05 m. Main polarizability (L1) decay curves are consistent and tightly distributed. Secondary polarizability (L2, L3) decay curves are relatively stable and could be used for classification in most cases. This suggests a strong potential for reliable classification of 37 mm projectiles.

The relative performance of the MPV and MPV2 sensor designs are illustrated by the simulation results in Figure 37 and Figure 38. The same nine-point pattern, 0.6-m station spacing – which results in 0.2 m sampling with both systems – and survey errors of 2 cm and 2 degrees were

applied to survey of 37 mm projectiles buried between 0.25-0.45 m. Stability of the main recovered parameters is similar with both sensors: depth is generally recovered within 0.05 m; the main polarizability (L1) is stable and its variability at all times is less 50% of its median value. Secondary polarizabilities are generally less stable, especially for the MPV2 for the deepest targets. Similar classification performance is expected using the stable L1 parameter.

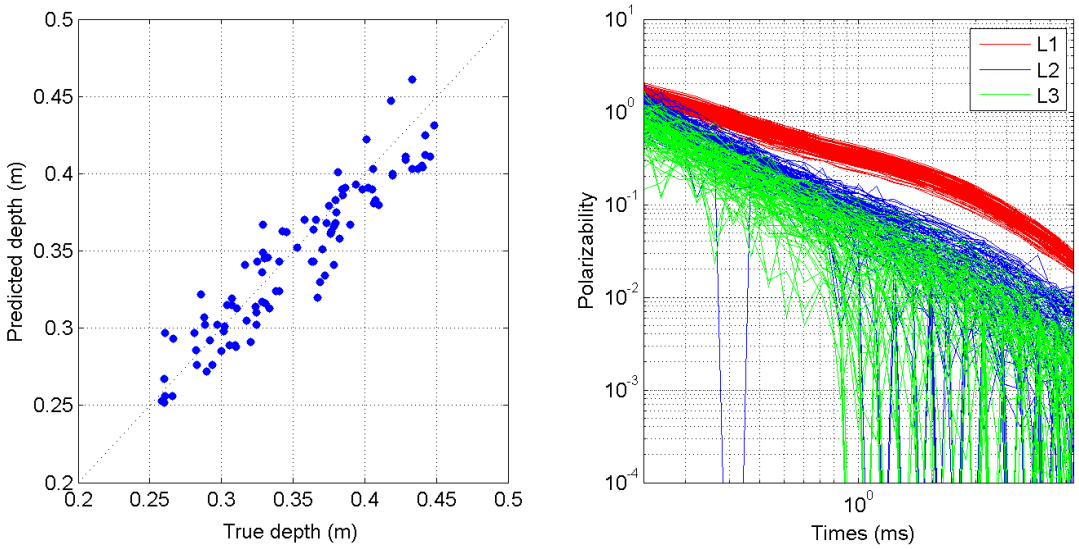

Figure 37: Simulated performance of MPV2 for the recovery of 37 mm projectiles. Survey errors are increased to 2 cm positional and 2 degree orientation error. Depth is recovered within 0.05 m. The main polarizability (L1) decay curves are consistent, although with larger variability than previous examples. Secondary polarizabilities are less constrained. Classification should mainly rely on stable L1 and still facilitate reliable and efficient discrimination performance.

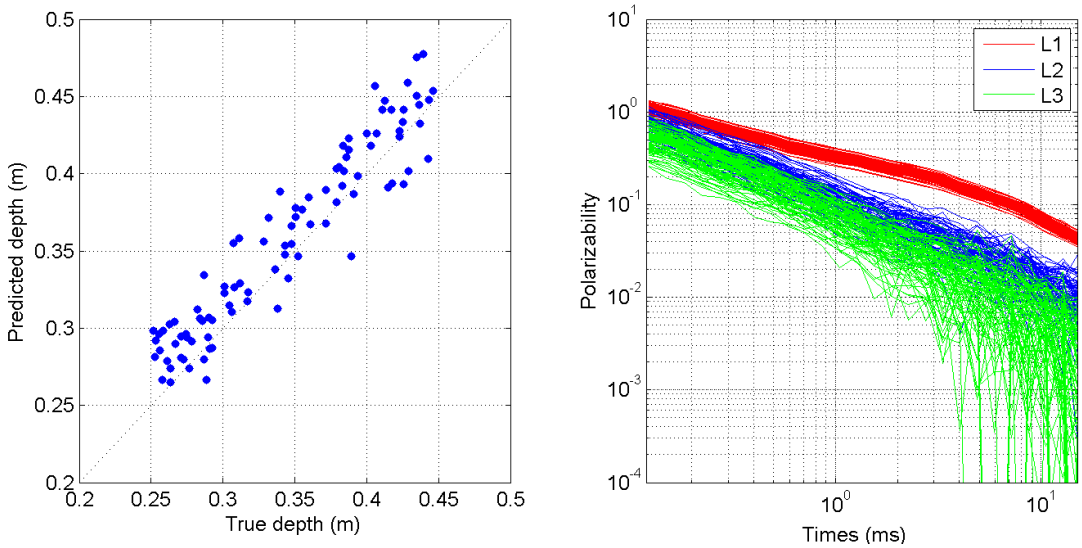

Figure 38: Simulated performance of the original MPV for the recovery of 37 mm projectiles. The same survey errors as those of Figure 37 are applied. Depth is recovered within 0.05 m. The main polarizability (L1) decay curves are consistent, although with some variability. Secondary polarizabilities are less constrained. Efficient classification is expected using L1.

The possibility to apply the MPV2 with a reduced five-point pattern is investigated in Figure 39 and Figure 40. Simulations were performed for a 37 mm projectile, using 2-cm and 2-degrees error. The depth and main polarizability parameters are generally stable, which suggests that reliable classification would remain possible in these conditions.

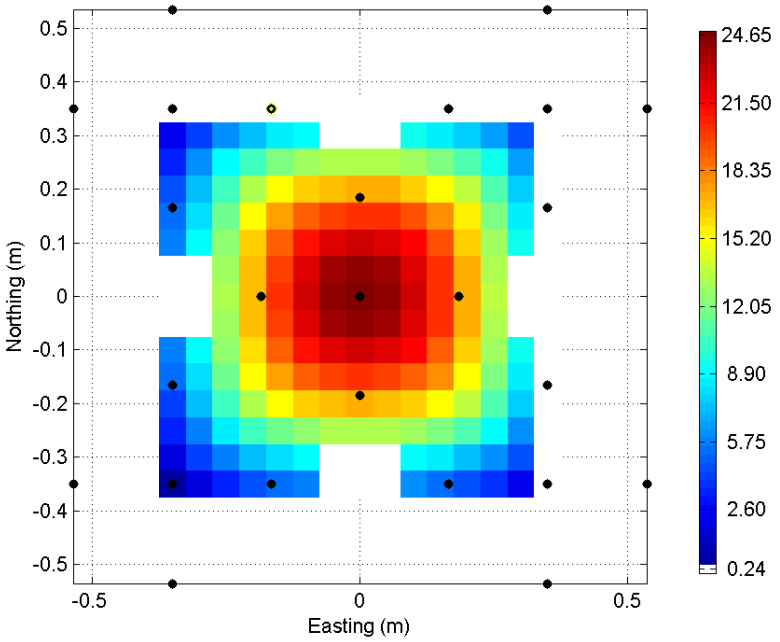

Figure 39: Five-point survey pattern with new MPV2. Station spacing is 0.35 m. Data from Z-component of the center receiver are gridded.

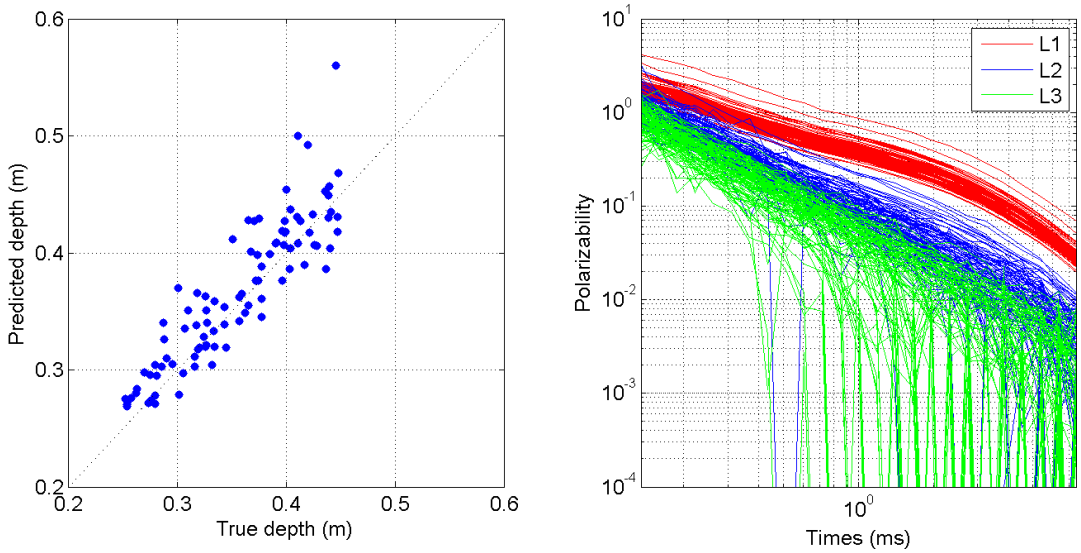

Figure 40: Simulated performance of MPV2 for the recovery of 37 mm projectiles. The survey pattern is reduced to 5 points shown in Figure 39. Survey errors are distributed with 2 cm positional and 2 degree orientation standard deviation. Depth is recovered within 0.05 m in most case and degrades to 0.12 m at most. The main polarizability (L1) decay curves remain consistent, although with larger variability than previous examples. Secondary polarizabilities are less well

constrained. Classification should mainly rely on the stable L1 polarizabilities and should still facilitate reliable and efficient discrimination performance.

Overall, this series of simulations show that stable parameter recovery for 37 mm projectiles and 81 mm mortars could be obtained for simulated data with the new MPV2 design within, and possibly beyond, the commonly accepted 11-times-target-diameter investigation depth. This analysis suggests that the proposed MPV2 design theoretically meets the data quality requirements for a UXO classification sensor.

D.5 Beacon positioning with MPV and MPV2

The effect on the beacon positioning accuracy is also minor: the primary field amplitude is reduced by approximately a factor 3 or 9.5 dB at all distances (see near-surface contours in Figure 31). Simulations were performed with the two sensor designs. Results are shown in Figure 41 and Figure 42.

We assumed a zigzag type of survey as the operator walked away from the beacon receiver boom, and variations in the height, roll and pitch as the sensor swung from side to side. The beacon receiver units were separated by 2 m. We also assumed that the two MPVs had similar current waveform and noise characteristics. Our analysis suggests that the 1-2 cm accuracy-level range would be reduced from 5 m to 4 m when moving to a smaller MPV. Actual tests with the new sensor head confirmed adequate accuracy within the 3-4 m range, which is sufficient for field operation.

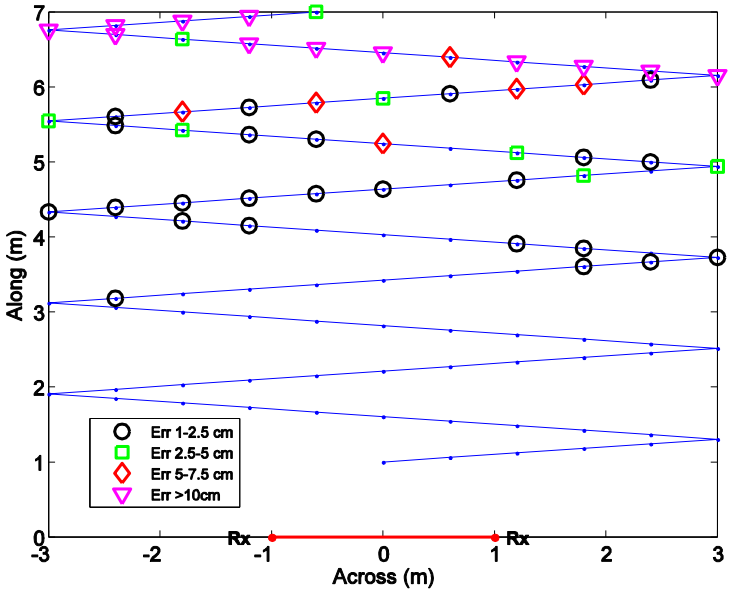

Figure 41: Simulation of beacon positioning accuracy range for original MPV. The beacon boom is indicated with the red line and dots and the bottom. Circles indicate positional error exceeding 1 cm.

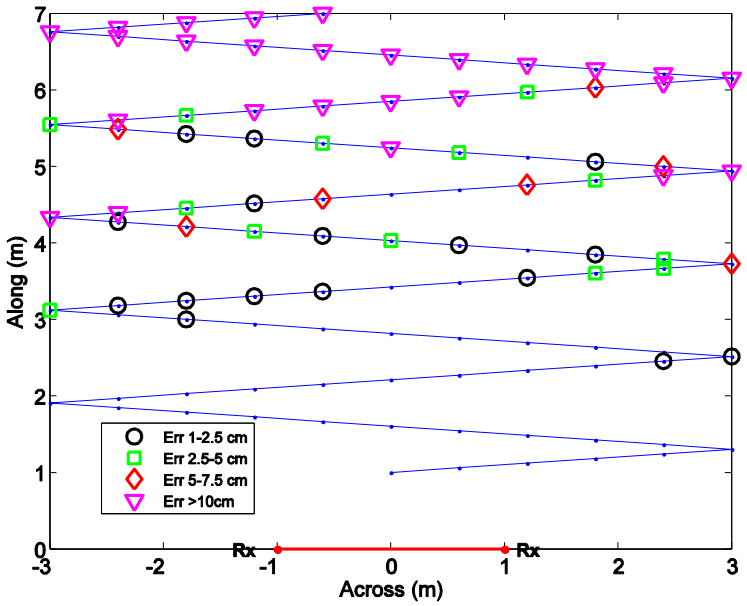

Figure 42: Simulation of beacon accuracy range for 0.5 m diameter MPV2.

D.6 Conclusion

Redesign of the original MPV sensor was indispensible for allowing practical field operation. Ruggedness and maneuverability had to be improved by reducing the sensor weight and size while high data quality had to be maintained. Based on COTS available material we found a compromise that allowed for a 50% reduction in the sensor head weight and 40% reduction in diameter. The new casing protects the EMI components; its round, smooth shape makes it less likely to snag on obstacles; it is transparent, allowing the operator to see through it to the ground. Updated EMI components have reduced the sensor noise. Although geometrically smaller, the new sensor design is expected to preserve the UXO detection and discrimination performance objectives and the capability to use the beacon positioning method.